

## Review

# Hygroscopic polymer gels toward atmospheric moisture exploitations for energy management and freshwater generation

Feng Ni,<sup>1,2</sup> Peng Xiao,<sup>1,2,\*</sup> Chang Zhang,<sup>1,2</sup> and Tao Chen<sup>1,2,\*</sup>

## SUMMARY

Atmospheric moisture exploitation (AME) technology has emerged as a promising alternative solution to improve the unbalanced supply-and-demand relationship between reducing essential resources (particularly energy and freshwater) and growing population. In this regard, emerging hygroscopic polymer gels (HPGs) are regarded as desirable materials for AME owing to their considerable hygroscopicity, highly tuneable structures, and easy integration with functional components. This review covers an in-depth and all-around overview of the up-to-date progress in HPGs used for AME. Firstly, the hygroscopic mechanisms of HPGs are revealed, followed by the presentation of state-of-the-art construction strategies, and the relationships between structures and properties are illustrated in detail. Furthermore, diverse cutting-edge applications based on HPGs for energy management and freshwater generation are also introduced, including fuel production, thermal dissipation, electric generation, hydrochromism, freshwater collection, and agricultural irrigation. Finally, we outline current challenges and their development trends of HPGs in AME applications in the coming future.

## INTRODUCTION

More than 7 billion people live on this planet now, and this number is projected to increase to almost 10 billion by 2050.<sup>1,2</sup> Such an explosive rise in the global population has created a huge demand for energy and freshwater, which are essential resources closely related to human life.<sup>3–5</sup> Although extensive efforts have been dedicated to exploring new technologies, there are still significant challenges to achieving energy and freshwater sustainability.<sup>6</sup> As expected, energy and freshwater provision will come under tremendous pressure in the foreseeable future, which may trigger severe conflicts and even threaten human lives.<sup>7–9</sup> Therefore, it becomes imperative to explore new resources and additional technologies to further complement existing production methods to generate energy and freshwater.<sup>6,10,11</sup>

Owing to the global hydrological cycle, a huge and ubiquitous water source exists in the atmosphere, in the form of clouds, drops, and vapor<sup>12</sup> (Figure 1A). Among them, atmospheric moisture is the most reliable resource as it exists everywhere regardless of climatic conditions. It is estimated that it can reach up to 12,900 cubic kilometers, six times the total volume of global rivers, at all time,<sup>13,14</sup> which can satisfy all demands of humans for energy and freshwater if it is well utilized. Unfortunately, atmospheric moisture is often overlooked. In this respect, atmospheric moisture exploitation (AME) technology is a promising alternative to realizing energy and freshwater sustainability.<sup>6,14–18</sup> Moreover, AME can also provide a decentralized strategy for

## PROGRESS AND POTENTIAL

Sustainable provisions of energy and freshwater have substantial implications for society's development and have become global hotspots. As an alternative water source, atmospheric moisture holds significant potential for decentralized water and/or energy generation regardless of geographical and hydrologic conditions. Emerging hygroscopic polymer gels (HPGs) characterized by 3D crosslinked polymeric networks have been intensively designed to achieve considerable atmospheric moisture trapping and storage. Moreover, rational integrations of functional additives into their networks through gelation chemistry allow HPGs versatile properties to exploit captured moisture for various frontier energy- and water-related applications, such as fuel production, thermal dissipation, electric generation, hydrochromism, freshwater collection, and agricultural irrigation. In this review, we also discuss the moisture sorption mechanisms of HPGs in detail, illustrate their relevant construction strategies, and finally outline their challenges and opportunities in this stage.

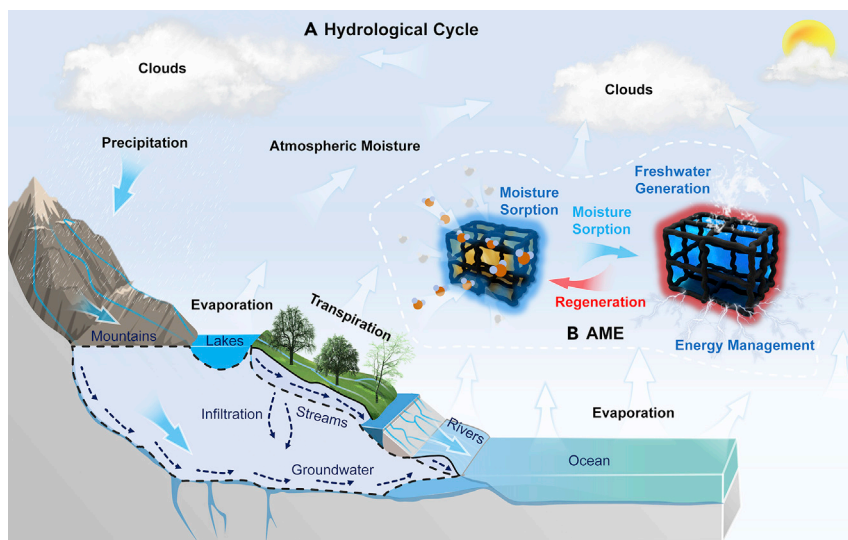


**Figure 1. Schematic of AME**

(A) The abundant moisture resources enabled by the global hydrological cycle on Earth.  
(B) The working principle of the sorption-based AME for energy management and freshwater generation, involving moisture sorption and utilization of captured moisture.

isolated off-grid areas to yield energy and freshwater without geographical and climatic constraints.<sup>6,14–19</sup>

Specifically, atmospheric moisture harvesting (AMH) is the primary step in the AME. Versatile AMH strategies, including fog collection, dewing, and sorption, have been developed in past decades.<sup>12,19–22</sup> Fog collection, referring to the harvesting of tiny droplets in the air, however, heavily depends on weather conditions, as it needs the emergence of fog.<sup>23,24</sup> In addition, dewing is another approach that can condense moisture via cooling the temperature below the dew temperature of water. Despite its high efficiency, intensive energy with high cost will be consumed, which is uneconomical and inaccessible in practical usage.<sup>12</sup> By comparison, sorption technology can spontaneously trap moisture using sorbents with well-established chemical and physical structures without weather limitations or energy requirements.<sup>14–17</sup> As a result, the sorption strategy offers a new prospect for AMH in a more available and energy-efficient way.

As depicted in Figure 1B, there are two cyclic steps involved in a sorption-based AME; that is, moisture sorption and utilization of captured moisture. More specifically, the sorbents can spontaneously capture moisture from the air, store it, and then transform the captured moisture for energy harvesting and freshwater generation. In this process, the sorbent materials play a vital role, and their inherent properties, such as hygroscopicity and structures, as well as functionality, all affect the overall AME performances.<sup>14–18</sup> Therefore, the development of novel sorbent materials with higher hygroscopicity, well-made structures, and stronger functions, is a straightforward, effective, and attractive way for the blooming of the AME field.

Benefiting from highly tuneable physical structures and chemical properties, hygroscopic polymer gels (HPGs) can be precisely controlled by gelation chemistry to desirable hygroscopic performances.<sup>6,14</sup> Moreover, their rich porous structures and unique swelling properties enable HPGs to act as reservoirs for captured water storage without leakage.<sup>25</sup> Furthermore, the easy integration of functional additives

<sup>1</sup>Key Laboratory of Marine Materials and Related Technologies, Zhejiang Key Laboratory of Marine Materials and Protective Technologies, Ningbo Institute of Materials Technology and Engineering, Chinese Academy of Sciences, Ningbo 315201, China

<sup>2</sup>School of Chemical Sciences, University of Chinese Academy of Sciences, Beijing 100049, China

\*Correspondence: [xiaopeng@nimte.ac.cn](mailto:xiaopeng@nimte.ac.cn) (P.X.), [tao.chen@nimte.ac.cn](mailto:tao.chen@nimte.ac.cn) (T.C.)

<https://doi.org/10.1016/j.matt.2022.06.010>

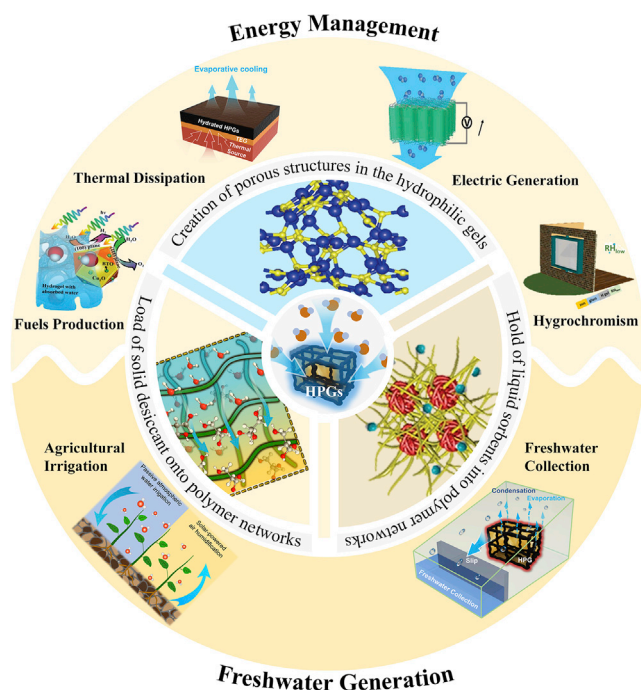


**Figure 2.** Summary of design strategies of HPGs and their AME applications

in the HPGs allows them versatile properties to further utilize captured moisture for various energy and/or water harvesting.<sup>6,26–28</sup> Therefore, HPGs have emerged as a desirable platform material used in AME during the past years.

At present, AME technologies based on HPGs are still evolving at an incredible rate, but remain in their early stages. Although considerable encouraging advances have been achieved, there is still no review to systematically summarize the latest development in HPGs and their promising AME applications for energy management and freshwater generation. Therefore, this timely review covers a comprehensive overview of such emerging hygroscopic materials for HPGs for AME. In this review, we start by analyzing the moisture sorption mechanisms of HPGs, followed by discussing versatile fabrication strategies, including but not limited to the creation of porous structures in the hydrophilic gels, mixing hygroscopic components (e.g., solid desiccants and liquid sorbents) within polymer networks, and demonstrate their structure-property relationships. Then we present the development of HPGs in many cutting-edge AME technologies for energy management and freshwater generation, involving fuels production, thermal dissipation, electric generation, hydrochromism, freshwater collection, and agricultural irrigation (Figure 2). Finally, we summarize the challenges and prospects of HPGs at this stage. We strongly hope that such booming innovations of HPGs illustrated in this review can push forward the frontiers of AME technology, finally contributing to the vision of sustainable development.

### DESIGN AND CONSTRUCTION OF HPGs

The essential step to trigger AME is to capture moisture from the atmosphere. In this regard, dominant criteria, such as equilibrium sorption capacity (ESC) and sorption kinetics, have been applied to design and construct desirable HPGs for considerable moisture sorption.<sup>14,16,17</sup> First of all, the ESC of HPGs is a curial factor in evaluating their hygroscopicity, because it determines the maximum amounts of water

available in the later AME.<sup>29</sup> Typically, the ESC of the HPGs was measured by dynamic moisture sorption, which can give the equilibrium moisture uptake as a function of the relative humidities (RHs) at a specific temperature. The sorption kinetics is another primary consideration for HPGs in serving as moisture sorbents, which strongly depends on their structural configurations and surface properties.<sup>30,31</sup> For HPGs, by faster sorption kinetics is meant a larger moisture sorption amount in a given time under the same RH and temperature. On some application occasions, rapid sorption kinetics of HPGs can allow them to realize multiple sorption-desorption cycles in 1 day, resulting in more water collection.<sup>30,32</sup> However, these two factors should be comprehensively considered as per their application conditions for HPGs to achieve desirable moisture sorption. To date, various state-of-the-art HPGs have been obtained through diverse material designs and fabrication strategies. In this section, the underlying moisture sorption mechanisms of HPGs are first be discussed in detail. Moreover, relevant advances in the designs and constructions of HPGs are also introduced along with representative samples. In addition, an all-round summary of recently developed HPGs, including their classifications, design and fabrication strategies, hygroscopic performances, advantages, and current challenges, are given in [Table 1](#) as a guide for their following developments.

### Moisture sorption mechanisms of HPGs

Understanding their moisture sorption mechanisms can provide a better design principle for the construction of desirable HPGs. For the moisture sorption process, in general, two processes occur simultaneously inside the HPGs, namely, moisture trapping and water storage. Specifically, moisture trapping takes place on the gas-solid interface of HPGs, resulting from various interactions between water molecules and HPGs ([Figure 3A](#)). Hence, according to different interactions, moisture sorption can be categorized into physisorption and chemisorption, respectively. Physisorption is mediated by van der Waals force, which is a rapid and reversible process. The Brunauer, Emmett, and Teller (BET) isotherm, a mainstream model, is developed to explain physisorption based on a certain hypothesis,<sup>14,46</sup> and the corresponding BET equation is described by [Equation 1](#):

$$\frac{1}{v[(p_0/p) - 1]} = \frac{c - 1}{v_m c} \left(\frac{p}{p_0}\right) + \frac{1}{v_m c}, \quad (\text{Equation 1})$$

where  $p_0$  and  $p$  are the saturation pressure and the partial pressure of water vapor at the given sorption temperature, respectively;  $v$  is the equilibrium amount of water molecules at the  $p/p_0$ ;  $v_m$  refers to the monolayer water molecules amount;  $c$  is the BET constant, which is calculated by [Equation 2](#):

$$c = \frac{\exp(E_1 - E_n)}{RT}, \quad (\text{Equation 2})$$

where  $E_1$  is the sorption enthalpy for the first layer, and  $E_2$  is the that for the second and higher layers;  $R$  is the gas constant and  $T$  is the sorption temperature. As a result, the surface texture of HPGs plays an important role in their physisorption, where a large surface area ( $v_m$ ) is beneficial to achieve a higher sorption capacity ( $v$ ). Moreover, owing to its weak affinity to water molecules, physisorption has a low sorption enthalpy of  $\sim 20$  kJ/mol or less, and thus allows a low energy barrier to release the captured water.<sup>14,32,47</sup> For hydrophilic HPGs, chemisorption causes moisture trapping through stronger chemical interactions, such as hydrogen bonds, electrostatic interactions, and coordination effect. In this regard, the Langmuir isotherm model is introduced to explain the chemisorption behavior, and obeys the following equation:



**Table 1. Summary of recently developed HPGs for moisture sorption**

Fabrication	Representatives	Hygroscopic performance	Advantages	Current challenges
<b>Design: IPGs creation of porous structures in the gels</b>				
sol-gel transformation	silica gel <sup>33</sup>	0.45 g g <sup>-1</sup> at 100% RH, 25°C	well-studied, commercial availability	low moisture uptake
sol-gel transformation	SNHG <sub>s</sub> <sup>32</sup>	3.6 g g <sup>-1</sup> at 90% RH, 25°C for 12 h	high moisture uptake in high RHs, low regeneration temperature	low moisture uptake in low RHs
sol-gel transformation	Cu-complex hydrogel <sup>34</sup>	0.2 g g <sup>-1</sup> at 40% RH, 20°C; 0.6 g g <sup>-1</sup> at 60% RH, 20°C; 1.25 g g <sup>-1</sup> at 80% RH, 20°C; 3.05 g g <sup>-1</sup> at 95% RH, 20°C	high moisture uptake in high RHs, low regeneration temperature	low moisture uptake in low RHs
sol-gel transformation	Co-SHM <sup>35</sup>	0.11 g g <sup>-1</sup> at 30% RH, 25°C; 0.83 g g <sup>-1</sup> at 60% RH, 25°C; 4.50 g g <sup>-1</sup> at 95% RH, 25°C	high moisture uptake in high RHs, low regeneration temperature	low moisture uptake in low RHs
freeze drying	PGF <sup>30</sup>	0.64 g g <sup>-1</sup> at 60% RH, 25°C; 4.20 g g <sup>-1</sup> at 90% RH, 25°C; 5.20 g g <sup>-1</sup> at 100% RH, 25°C	high moisture uptake in high RHs, rapid sorption/desorption kinetics	low moisture uptake in low RHs, structural stability
freeze drying	G-PDDA <sup>31</sup>	0.13 kg kg <sup>-1</sup> at 30% RH, 25°C; 0.37 kg kg <sup>-1</sup> at 60% RH, 25°C; 1.1 kg kg <sup>-1</sup> at 90% RH, 25°C	high moisture uptake in high RHs, rapid sorption/desorption kinetics	low moisture uptake in low RHs, structural stability
<b>Design: MPGs load of solid desiccant onto polymer networks</b>				
immersion drying	PAM-CNT-CaCl <sub>2</sub> <sup>36</sup>	0.69 g g <sup>-1</sup> at 30% RH, 25°C; 1.08 g g <sup>-1</sup> at 60% RH, 25°C; 1.73 g g <sup>-1</sup> at 80% RH, 25°C	high ESC	slow sorption/desorption kinetics, corrosive
immersion drying	Alg-CaCl <sub>2</sub> <sup>37</sup>	1.18 g g <sup>-1</sup> at 33% RH, 28°C; 1.59 g g <sup>-1</sup> at 56% RH, 28°C; 2.26 g g <sup>-1</sup> at 78% RH, 28°C	high ESC	slow sorption/desorption kinetics, corrosive
immersion drying	PDMAPS-LiCl <sup>38</sup>	0.62 g g <sup>-1</sup> at 30% RH, 30°C	high ESC	slow sorption/desorption kinetics, corrosive
freeze drying and immersion drying	vertically aligned LiCl@rGO-SA <sup>39</sup>	1.01 g g <sup>-1</sup> at 15% RH, 30°C; 1.52 g g <sup>-1</sup> at 30% RH, 30°C	high ESC, rapid sorption/desorption kinetics	structural stability
ions exchange	Bina <sup>40</sup>	5.6 g g <sup>-1</sup> at 70% RH, 25°C for 700 min	high ESC	slow sorption/desorption kinetics, corrosive
ions exchange	PAETA-Ac <sup>41</sup>	0.87 g g <sup>-1</sup> at 80% RH;	none-corrosive	slow sorption/desorption kinetics
impregnation network	SAMG <sup>42</sup>	0.70 g g <sup>-1</sup> at 30% RH, 25°C; 0.40 g g <sup>-1</sup> at 60% RH, 25°C; 6.70 g g <sup>-1</sup> at 90% RH, 25°C	thermo-responsive water oozing, high ESC	high cost

(Continued on next page)

Table 1. Continued

Fabrication	Representatives	Hygroscopic performance	Advantages	Current challenges
<i>in situ</i> copolymerization and immersion drying	PC-MOF <sup>43</sup>	0.76 g g <sup>-1</sup> at 30% RH, 25°C for 12 h; 1.61 g g <sup>-1</sup> at 60% RH, 25°C for 12 h; 3.74 g g <sup>-1</sup> at 90% RH, 25°C for 12 h	autonomous water oozing, high ESC	high cost
Design: MPGs hold of liquid sorbents into polymer networks				
solvent displacement	POG <sup>44</sup>	16.01 kg m <sup>-2</sup> at 90% RH, 25°C	high ESC	relatively slow sorption/desorption kinetics
<i>in situ</i> copolymerization	RIG <sup>45</sup>	1.25 g g <sup>-1</sup> at 90% RH, 25°C	high ESC, strong adhesion	relatively slow sorption/desorption kinetics

$$\theta = \frac{Kp_m}{1 + Kp_m}, \quad (\text{Equation 3})$$

where  $\theta$  is the equilibrium fraction of sorption sites occupied, which can reflect the chemisorption capacity in a sense,  $K$  is the equilibrium constant depending on the intrinsic affinity of the sorbents to water molecules and temperature, and  $p_m$  is the partial pressure of moisture. Therefore, a stronger interaction between sorbents and water molecules (a larger  $K$ ) and higher environmental humidity (a larger  $p_m$ ) are both desirable for improving chemisorption according to the Langmuir isotherm model. However, a higher affinity of chemical interactions for sorbents usually results in a greater barrier to their regeneration. Therefore, there is a trade-off between efficient moisture sorption and easy regeneration in designing HPGs. In this sense, hydrogen bonds with suitable bonding energy (9.7–29.0 kJ/mol) are highly preferable in HPGs,<sup>16</sup> which is higher than that of physical van der Waals forces and enables HPGs to take up moisture in low RHs. However, the bonding energy in hydrogen bonds is weaker than that of other chemical bonds for easy activation, thus striking a balance between moisture sorption and regeneration. Moreover, the increment of sorption sites of HPGs can also effectively improve their chemisorption. In this respect, the enlargement of the sorption area via creating porous structures inside HPGs has been a general strategy to further promote their sorption.<sup>30,31</sup>

In addition, water storage usually occurs in the HPGs after moisture trapping. In light of different storage modes, there are two sorption behaviors for HPGs, namely, adsorption and absorption. Adsorption is an exothermic moisture sorption process that only appears on the surface of HPGs,<sup>19</sup> which is greatly influenced by their interacting forces and areas with water molecules (Figure 3B). Moreover, for porous HPGs, moisture adsorption occurs not only on their bulk surface but in their pore structure. As demonstrated in Figure 3C, the moisture can be adsorbed by porous HPGs in two ways, including pore filling or capillary condensation.<sup>16,48,49</sup> Typically, the smaller pore diameters can effectively promote the adsorption potential of HPGs to achieve their moisture adsorption at lower RHs.<sup>16,48,49</sup> When their effective pore diameter is lower than the critical diameter ( $D_c$ ) of the water, HPGs can undergo moisture adsorption through pore filling.<sup>48,49</sup> The  $D_c$  of water is calculated as follows:<sup>46,49,50</sup>

$$D_c = \frac{4\sigma T_c}{(T_c - T)}, \quad (\text{Equation 4})$$

in which  $\sigma$  is the van der Waals diameter of the water molecule ( $\sim 2.8$  Å), and  $T_c$  ( $\sim 647$  K for bulk water) and  $T$  refer to critical temperature and the adsorption temperature of the water, respectively. As a result, the  $D_c$  of the water is  $\sim 2.076$  nm

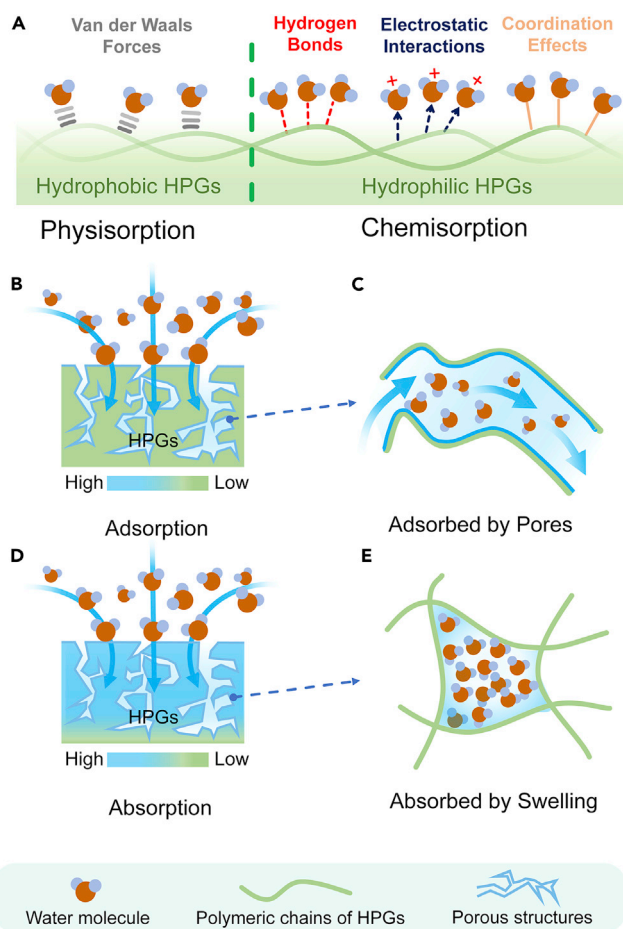


**Figure 3. The moisture sorption mechanisms for HPGs**

(A) Physisorption and chemisorption of HPGs.

(B) Adsorption behavior of HPGs.

(C) The captured water was adsorbed by their pores.

(D) Absorption behavior of HPGs.

(E) The captured water was absorbed by swelling.

at 25°C. Thus, for HPGs with hydrophilic properties, the adsorbed water molecules will firstly nucleate on their hydrophilic sites, which can continuously act as new adsorption sites to trap water molecules for the formation of small water clusters, finally leading to a continuous pore filling.<sup>16</sup> It is worth noting that the primary moisture adsorption is chemisorption due to hydrophilic groups of HPGs, but subsequent adsorption is mainly on physisorption, therefore requiring less energy for their regeneration.<sup>47</sup> In addition, hydrophobic HPGs with a pore size smaller than  $D_c$  for moisture adsorption mainly depend on van der Waals forces, and the pore filling will start at the pore center.<sup>50</sup> Owing to their hydrophobicity and pore diameters, the above HPGs generally demonstrate a very limited hygroscopicity, and thus none have been reported so far. Moreover, for HPGs with pore sizes larger than  $D_c$ , capillary condensation will occur when their critical condensation pressure is reached.<sup>16,48</sup> According to the Kelvin equation, the critical condensation pressure of HPGs is determined by their pore diameters.<sup>16,51</sup> Compared with pore filling, capillary condensation usually happens at higher RHs. However, the capillary condensation for HPGs can lead to a higher ESC than that of those with pore filling due to their larger pore volumes.

Furthermore, for most HPGs, there is an absorption behavior, where water molecules are first captured by sorption sites on their surface and then further incorporated into their crosslinked polymeric networks through swelling (Figure 3D). Therefore, the absorption kinetics of HPGs is not only determined by their surface properties and texture structures but also depend on their swelling, in other words the liquid diffusion in their bulk.<sup>52,53</sup> Liquid diffusivity  $D_l$  in the HPGs can be described by Biot's linear theory of poroelasticity coupling the chemical potential gradient of captured water and the elastic energy of the HPGs, which can be defined as:

$$D_l = \frac{2Gk_0\phi_1(1+\nu)}{3\eta(1-2\nu)(1-\phi_1)^{1.5}} \quad (\text{Equation 5})$$

where  $G$  and  $\nu$  are the shear modulus and Poisson ratio of the HPGs, respectively,  $\eta$  is the dynamic viscosity of water,  $\phi_1$  is the local volume fractions of liquid in the HPGs, and  $k_0$  is a constant relating to the geometric properties of HPGs. As a result, a higher  $G$  and optimized initial solid fraction for HPGs is desirable for a faster inner liquid transport to improve their absorption kinetics. In this regard, recently, Díaz-Marín et al. developed a generalized two-concentration model coupling the vapor pressure difference and the water chemical potential gradient to identify key design parameters of HPGs for fast absorption kinetics, including their initial porosity, hydrogel thickness, and shear modulus.<sup>53</sup> Eventually, continuous moisture absorption will result in swelling behaviors of HPGs, thus contributing to a larger ESC (Figure 3E). Note that the limit of ESC for HPGs highly depends on their swelling ratio, where a larger volume expansion can lead to more space for holding captured water and achieving a larger ESC. Therefore, the swelling of HPGs highlights their advantages as framework materials for moisture sorption over other solid sorbents, which should be taken into more account in the following research.

However, there is a combined hygroscopic behavior in actual HPGs instead of singular adsorption or absorption behavior, in which physical structures and chemical interactions both play essential roles. Therefore, a better understanding of the moisture sorption mechanisms of HPGs is necessary to make more informed designs and fabrications to achieve desirable hygroscopic performances in the future.

### Intrinsic-type HPGs

When featured with well-designed chemical and/or physical structures, intrinsic-type polymer gels (IPGs) can directly harvest moisture from the air. Generally, polymer gels are fabricated from monomers or polymers through the formation of cross-linked networks. In this process, the chemical hydrophilicity of materials can enable themselves a remarkable hygroscopic ability. Therefore, the primary principle of HPGs preparation is tuning hydrophilic monomers or polymers to act as the backbones of IPGs. For example, polar groups such as hydroxyl (-OH),<sup>54</sup> amino (-NH<sub>2</sub>),<sup>55</sup> carboxylic acid (-COOH),<sup>30,56</sup> and sulfonic acid (-SO<sub>3</sub>H)<sup>57,58</sup> groups, etc., are commonly introduced into the networks of IPGs for moisture sorption, as they can form more abundant hydrogen bonds with water molecules. Moreover, charged ionic groups, including quaternary ammonium groups (NR<sup>3+</sup>) and acetate (Ac) groups (COO<sup>-</sup>), are also reported to help IPGs harvest moisture through forming electrostatic interactions with water molecules.<sup>31,56</sup> Furthermore, the metal sites on the backbones of IPGs can also provide coordination effects with water molecules and trap them.<sup>32,47,59,60</sup> In these cases, the amounts and the affinity of inherent hydrophilic groups on the IPG surface are both essential influencing factors for their hygroscopic performance. Typical examples of hygroscopic IPGs are hydrophilic cross-linked polymeric resins, such as the natural polymer (e.g., starch,<sup>61,62</sup> cellulose<sup>58</sup>)

and synthetic polymer (e.g., sodium polyacrylate,<sup>63</sup> polyvinyl alcohol [PVA],<sup>64</sup> phenolic resins<sup>54</sup>) xerogels, which have been widely developed and commonly employed for environment dehumidification,<sup>65</sup> sensors,<sup>66</sup> actuators,<sup>55,56,67</sup> etc. Even so, slow sorption kinetics of these IPGs caused by their dense network structures still result in unsatisfactory amounts of moisture sorption in a required time, which severely restrict their practical usage in energy and freshwater harvesting.

#### *Creation of porous structures in the hydrophilic gels*

From a mechanistic point of view, the physical porous structures cannot only enlarge the sorption surface,<sup>30,31,39</sup> but increase the sorption potential when a certain size is achieved.<sup>16,48,49</sup> Hence, it is usually designed in hydrophilic gels to promote their hygroscopic performances. For example, the sol-gel transformation is typical for constructing nanoporous inorganic IPGs. Among them, silica gels are one group of representative nanoporous materials with silanol groups on their surface, and have been intensively well studied and commercialized for moisture uptake<sup>33,68</sup> (Figure 4A). Unfortunately, silica gel usually shows a low moisture uptake due to its limited pore volumes and requires a high energy requirement for its regeneration, thus significantly restricting many applications.<sup>69</sup> Very recently, Nandakumar and co-workers presented super hygroscopic nanoporous hydrogels (SNHGs) via a similar strategy, which contained an amorphous non-stoichiometric compound of Zn and O atoms for a highly efficient moisture sorption<sup>32,47</sup> (Figure 4B). A nanoporous and fringed contour were present in the interior of the SNHGs with an optimized Zn/O ratio of 1:1.1, which significantly enhanced its adsorption surface. As a result, the SNHGs demonstrated a specific surface-area-dependent hygroscopic performance. When its specific surface area is  $350 \text{ cm}^2 \text{ g}^{-1}$ , such an SNHG could harvest over 360% of its weight for 12 h at 90% RH. Moreover, the corresponding density functional theory results also revealed that the binding energy of adsorbed water molecules with the SNHGs was initially high but then decreased sharply. The phenomenon indicated that the subsequent sorption was just physisorption, and thus less energy was required for its regeneration. As a result, such SNHGs exhibited a higher moisture uptake and a lower desorption barrier than other porous materials, such as silica gels and MOF-801 (Figure 4C).

Different from inorganic IPGs, organic hygroscopic IPGs enabled humidity harvesting through absorption strategy, which was capable of storing the captured water within their bulk polymeric mesh through swelling. In this regard, the common strategy for creating porous structures in these organic IPGs is freeze drying. For instance, Yao et al. recently proposed a porous sodium polyacrylate (PAAS)/graphene framework (PGF) for moisture uptake via freeze drying<sup>30</sup> (Figure 4D). The hygroscopicity of PGF was ascribed to the numerous -COOH groups localized on the PAAS, which could spontaneously form hydrogen bonds interacting with water molecules. Owing to the freeze drying process and the introduction of graphene oxide (GO), the PGF demonstrated microporous structures with pore sizes ranging from 30 to 50  $\mu\text{m}$  and porosity of up to 99%, which significantly promoted their sorption areas and inner vapor diffusion (Figure 4E). As a result, the PGF showed a faster sorption kinetics and a higher ESC than pure PAAS and GO (Figure 4F). Moreover, the PGF showed a great application potential in high RHs, enabling a superhigh ESC of  $5.20 \text{ g g}^{-1}$  at an RH of 100% (Figure 4G).

Another similar paradigm is the development of a hydrophilic aerogel material (G-PDDA) that is composed of a cationic polymer, poly-diallyl-dimethylammonium chloride (PDDA), with a negatively charged reduced GO (rGO) for moisture sorption<sup>31</sup> (Figure 4H). The abundant charged groups of  $\text{NR}^{3+}$  on PDDA could bond



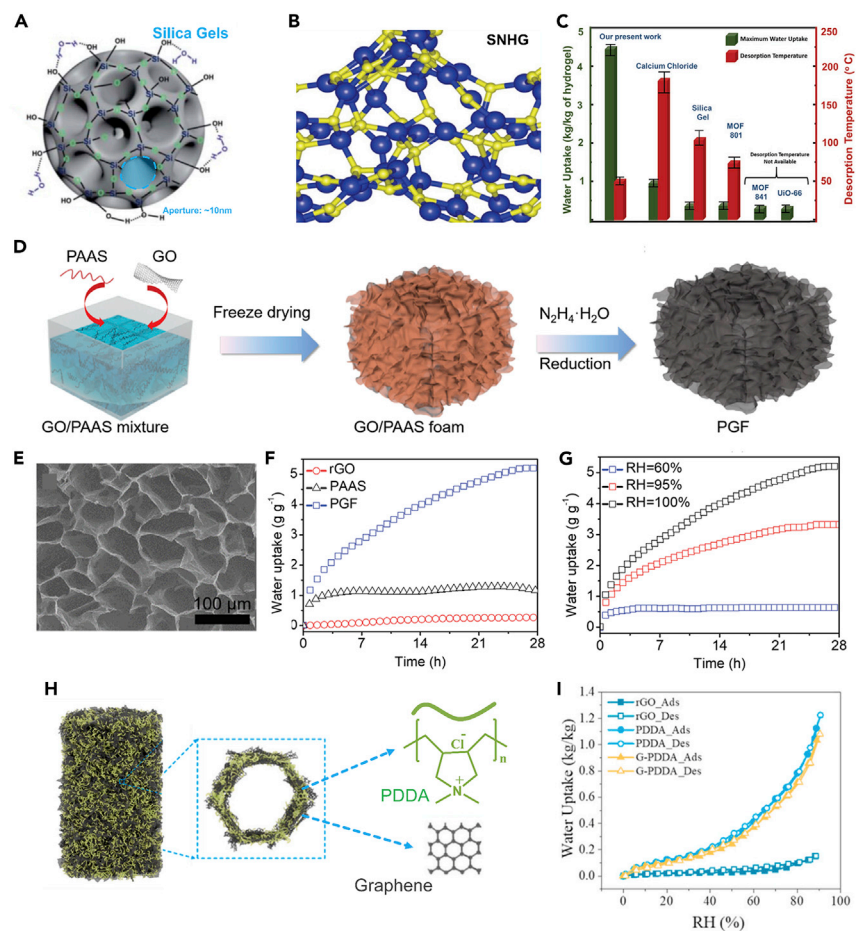


**Figure 4. Creation of porous structures in the hydrophilic gels**

(A) The nanoporous silica gel with hydrophilic groups. Reproduced with permission.<sup>68</sup> Copyright 2021, Royal Society of Chemistry.

(B) The simulated structure of the SNHG with an optimized Zn/O ratio of 1:1.1.

(C) A comparative chart showing the maximum ESC and desorption temperatures of reported hygroscopic materials. Reproduced with permission.<sup>32</sup> Copyright 2019, Wiley-VCH.

(D) Schematic of the fabrication of PGF.

(E) SEM image of PGF shows the cellular architecture.

(F) Moisture uptake of rGO, PAAS, and PGF for 28 h at 25°C and 100% RH.

(G) Moisture uptake of PGF under RHs of 60%, 95%, and 100%, respectively. Reproduced with permission.<sup>30</sup> Copyright 2020, Wiley-VCH.

(H) Schematic of physical and chemical structures of G-PDDA.

(I) Water sorption/desorption kinetics of PDDA and G-PDDA, measured at 25°C and 60% RH for uptake and 80°C and 4% RH for desorption. Reproduced with permission.<sup>31</sup> Copyright 2020, Elsevier.

with water molecules through electrostatic interactions, accounting for the hygroscopicity for G-PDDA and PDDA samples. Similarly, the addition of rGO in PDDA allowed G-PDDA to form a highly porous structure after freeze drying, which was conducive to realizing fast sorption/desorption kinetics. As shown in Figure 4I, pure PDDA takes about 20 h to reach its sorption equilibrium and 23 h to fully release water, but the G-PDDA takes only 20 min under the same conditions. Therefore, such a G-PDDA can harvest more moisture from the air by conducting multiple sorption-desorption cycles in a specific time than that of dense pure PDDA.

### Mixed-type HPGs

In addition, numerous existing hygroscopic materials, such as solid desiccants and liquid sorbents, can also be mixed with polymer gels to obtain mixed-type HPGs (MPGs) for moisture sorption. Generally, MPGs demonstrate a synergistically enhanced hygroscopicity compared with unmixed ones. Thus far, various accessible mixed approaches, including immersion drying,<sup>36,41,70,71</sup> ion exchange, impregnation network,<sup>42,72</sup> *in situ* copolymerization,<sup>45,73–75</sup> and solvent displacement,<sup>44</sup> have been developed to prepare hygroscopic MPGs.

#### *Loading of solid desiccant onto polymer networks*

The solid desiccants, including deliquescent salts, metal-organic frameworks (MOFs), silica gel, zeolite, etc., can provide open binding sites to bond with water molecules, and have been widely used for moisture uptake.<sup>14,16,17</sup> Therefore, a straightforward design to obtain HPGs is to immobilize solid desiccants onto polymer networks.

Owing to their multistep hydration processes, deliquescent salts, including lithium chloride (LiCl), calcium chloride (CaCl<sub>2</sub>), zinc chloride (ZnCl<sub>2</sub>), etc., can achieve a five to six times moisture sorption of their mass, which has gained enormous attention.<sup>14,76</sup> However, the liquefaction of these salts after deliquescence will result in many problems, such as leakage and aggregations as well as corrosion. In this sense, polymer gels can keep liquid in the form of solids and provide a swellable structure for liquid storage, enabling a promising matrix to combine with these deliquescent salts for moisture sorption.

The immersion drying method is regarded as a convenient approach to obtain MPGs loaded with salts as it does not require any complex modifications. As a proof-of-concept, Li et al. prepared an HPG by composing deliquescent CaCl<sub>2</sub> onto the polymer networks of polyacrylamide (PAM).<sup>36</sup> As shown in Figure 5A, the resultant PAM-CNT (carbon nanotube)-CaCl<sub>2</sub> was obtained by directly immersing PAM-CNT gel in CaCl<sub>2</sub> aqueous solution with subsequent drying. As a result, the PAM-CNT-CaCl<sub>2</sub> demonstrated a wide hygroscopic range and could realize an ESC of 5%, 69%, 110%, and 173% of self-weight with RHs of 10%, 35%, 60%, and 80%, respectively. Notably, the salt content can play an essential role in the hygroscopic performance of the salt composite HPGs. Generally, for HPGs with a large swelling ratio, higher salt content can enable larger water chemical potential differences to accelerate their swelling behavior, realizing a faster sorption kinetics in the initial stage and a larger equilibrium moisture uptake.<sup>53</sup> Unfortunately, for most gel materials, a salting-out effect will occur when they swell in salt solutions, resulting in an aggregation of polymer chains and suppressing their swelling capability, leading to a limited moisture sorption.<sup>77</sup> In this sense, zwitterionic polymeric backbones with a special salting-in effect can allow HPGs more salt loading for a better hygroscopic performance.<sup>38,77</sup> For example, Lei et al. developed a salt-responsive polyzwitterionic hydrogel (PDMAPS-LiCl) composed of poly [2-(methacryloyloxy)ethyl]dimethyl-(3-sulfopropyl)ammonium hydroxide hydrogel with LiCl for moisture harvesting.<sup>38</sup> Owing to its salting-in effects, the addition of LiCl enabled the PDMAPS chains with stretched conformation and enhanced mobility, improving the diffusion of captured water in the resulting hydrogel, especially under low RHs. As a result, the PAMPS-LiCl hydrogel demonstrated an enhanced hygroscopic performance of 0.62 g/g and impressive sorption kinetics of 120-min equilibrium time at 30% RH.

Recently, a new strategy known as “ions exchange” has come to light, in which a selective replacement of counterions in HPGs can efficiently promote their

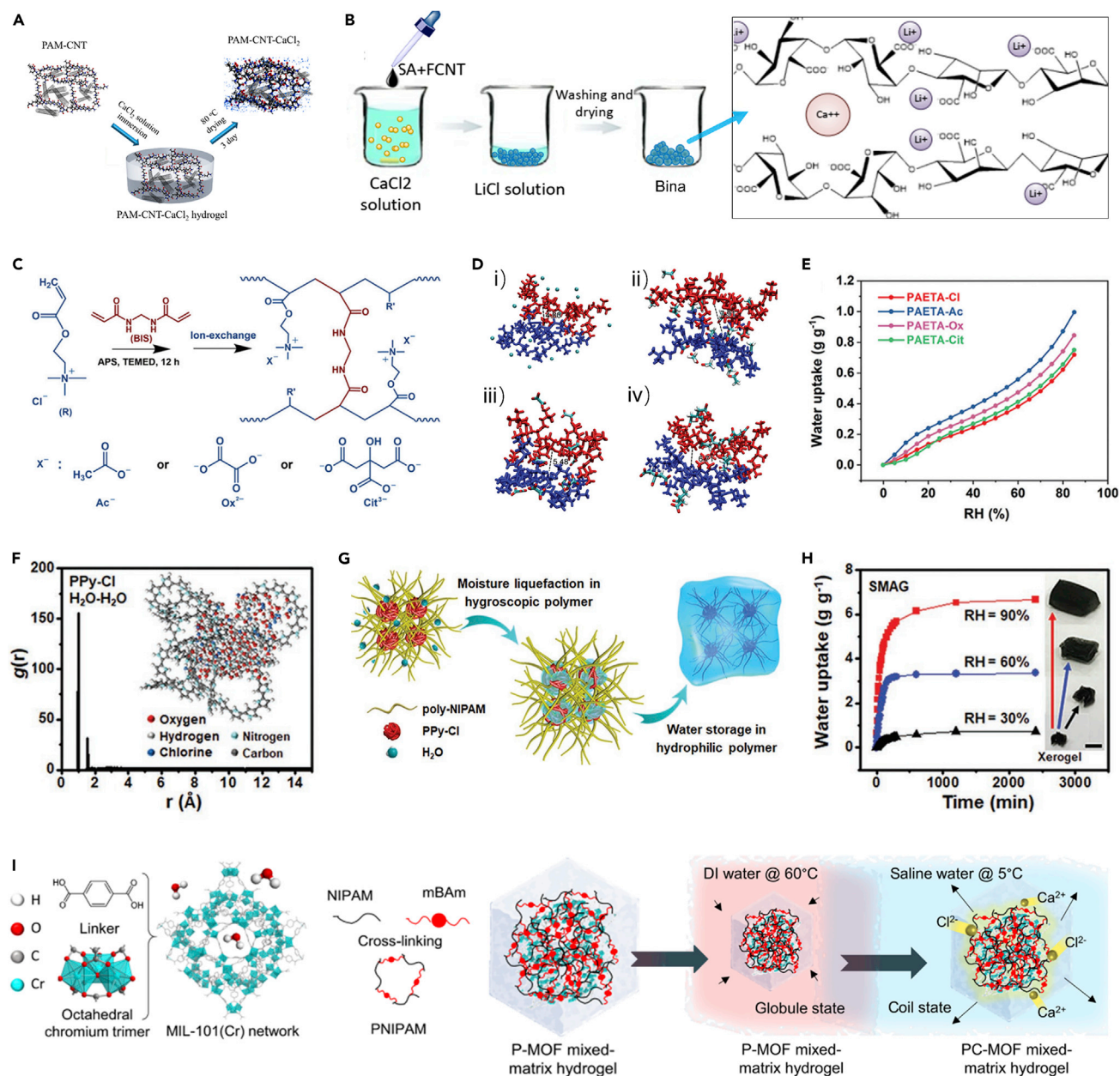


**Figure 5. Load of solid desiccant onto polymer networks**

(A) Schematic of the preparation of PAM-CNT-CaCl<sub>2</sub> hydrogel.<sup>36</sup> Copyright 2020, American Chemical Society.

(B) The fabricating strategy of Bina. Reproduced with permission.<sup>40</sup> Copyright 2020, American Chemical Society.

(C) The preparation and chemical structures of PAETA-X.

(D) Simulated results of different PAETA-X polymer chains that are bound with (i) Cl<sup>-</sup>, (ii) Ac<sup>-</sup>, (iii) Ox<sup>2-</sup>, and (iv) Cit<sup>3-</sup>.

(E) Moisture sorption isotherm curves of different PAETA-X. Reproduced with permission.<sup>41</sup> Copyright 2021, Royal Society of Chemistry.

(F) The molecular dynamic simulation of hygroscopic PPy-Cl absorbing moisture, and the insert is the computing model of hydrated PPy-Cl.

(G) Schematic of the moisture absorption enabled by the SMAG.

(H) Moisture uptake of SMAGs at different RHs of 30%, 60%, and 90%. Reproduced with permission.<sup>42</sup> Copyright 2019, Wiley-VCH.

(I) The preparation routes of the PC-MOF. Reproduced with permission.<sup>43</sup> Copyright 2020, AAAS.

hygroscopic performances. Entezari et al. have designed an alginate gel modified with binary salts (Bina) for moisture uptake.<sup>40</sup> The detailed fabrication of Bina is demonstrated in Figure 5B: Ca<sup>2+</sup> was first chosen to crosslink two G-blocks from

two sodium alginate chains, and then  $\text{Li}^+$  was applied to replace all remaining sodium ions on chains. Compared with the sorbents incorporated with a single salt, the Bina was found to have a remarkable improvement both in sorption kinetics and ESC. Finally, the Bina exhibited a high ESC of  $5.6 \text{ g}_{\text{water}}/\text{g}_{\text{sorbents}}$  at 70% RH, which was higher than that of the recently reported desiccants. In another example, Wu et al. synthesized metal- and halide-free hydrogels (PAETA-X) by polymerization followed by organic-ion exchange, whose charged polymeric backbones and paired organic anions were both hygroscopic components<sup>41</sup> (Figure 5C). By altering paired anions, the ESC of PAETA-X could be well controlled, and the corresponding mechanisms were verified using VMD and Multiwfn software (Figure 5D). The results revealed that chain mobility and free volumes of PAETA-X would be significantly improved with the introduction of Ac anions, which effectively promoted its moisture sorption. As a result, the PAETA-Ac demonstrated the highest water uptakes, resulting in  $\sim 0.87 \text{ g g}^{-1}$  at  $25^\circ\text{C}$  and 80% RH (Figure 5E).

This is expected to be a promising method to fabricate hygroscopic MPGs via the design of novel hygroscopic materials at the molecular level and combining them with polymer gels. For instance, Zhao et al. have developed a molecular hygroscopic chloride-doped polypyrrole (PPy-Cl), which can effectively liquefy water vapor by its solvation effect<sup>42</sup> (Figure 5F). The resulting hydrophilic PPy-Cl facilitated the formation of an interpenetrating structure with poly-NIPAM chains to obtain a super moisture-absorbent gel (SMAG). As demonstrated in Figure 5G, the moisture sorption mechanism of SMAG could be explained as follows: (1) moisture molecules were captured and liquefied to drops assisted by PPy-Cl and (2) water droplets were further transferred into its polymeric networks for storage. Thus, the SMAG exhibited impressive moisture sorption of 6.7, 3.4, and  $0.7 \text{ g g}^{-1}$  of corresponding dried samples at RHs of 90%, 60%, and 30%, respectively (Figure 5H).

In addition, the *in situ* copolymerization is regarded as a feasible approach to combine hygroscopic nanoporous solids, including MOFs, silica gels, and zeolite, with polymer gels to achieve MPGs. Recently, Yilmaz et al. proposed a MOF-assisted hygroscopic polymer gel (PC-MOF) for atmospheric moisture uptake.<sup>43</sup> Owing to its remarkable structure stability, high ESC, and fast sorption kinetics, MIL-101(Cr) was chosen in this system to blend with the polymeric mesh of poly-NIPAM through the *in situ* free-radical copolymerizations (Figure 5I). As expected, the highly hygroscopic MIL-101(Cr) could stably attach to the polymer networks for an improved moisture uptake. Furthermore, the PC-MOF was eventually obtained from P-MOF through a salinization process with the  $\text{CaCl}_2$  solution. As a result, a rapid uptake kinetics was also achieved at 90% RH for the PC-MOF, whose sorption rates could reach  $0.72 \text{ g g}^{-1} \text{ h}^{-1}$  within the first 3 h. Moreover, the PC-MOF presented high-capacity sorption of up to  $5.27 \text{ g g}^{-1}$  after a 72-h continuous water harvest in 90% RH.

#### Hold of liquid sorbents into polymer networks

Liquid sorbents can provide a lower equilibrium water vapor pressure than the environment, thus demonstrating a hygroscopic capability from the air. To date, common hygroscopic liquid systems, including ionic liquids,<sup>78</sup> organic alcohols,<sup>79</sup> and concentrated salt solutions,<sup>80</sup> have been employed for moisture capture, which can absorb moisture into the whole volume driven by the concentration differences, and thus exhibit a favorable feature of continuous and large-capacity moisture harvest. However, due to their flowable characteristic, liquid sorbents still have some drawbacks in actual operations, such as potential leakage risk and poor portability. Furthermore, the restricted exposure surface of liquid sorbents also results in a limited hygroscopic performance. In this sense, polymer gels have superb



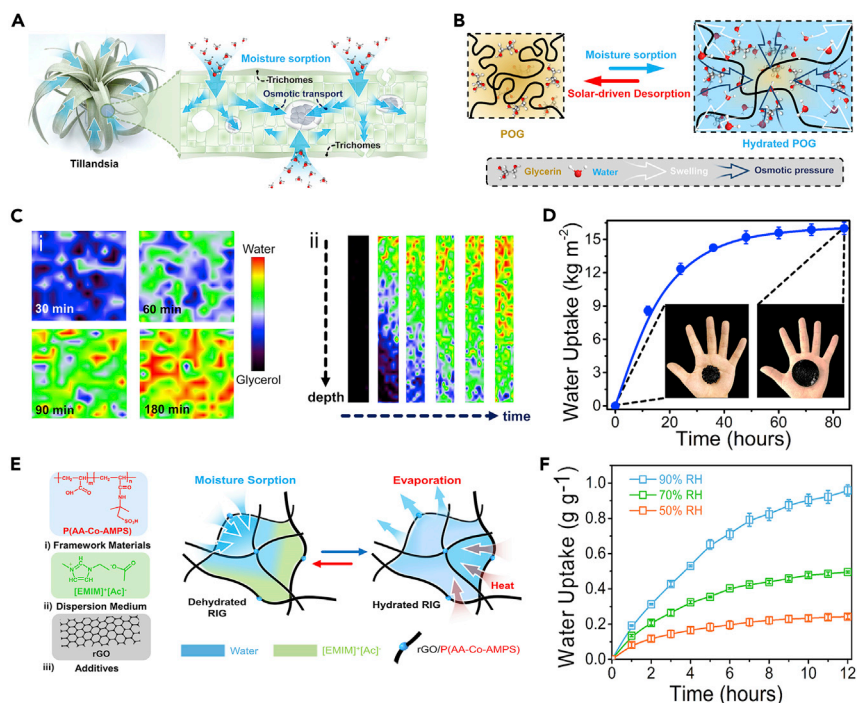


**Figure 6. Hold of liquid sorbents into polymer networks**

(A) Schematic illustration of water management of *Tillandsia* leaves.

(B) The moisture sorption mechanisms of the POG.

(C) 2D Raman mapping of (i) the surface and (ii) the interior of POG during moisture sorption.

(D) The moisture sorption equilibrium curve of POG; the inserts are the physical photos of POG before and after moisture sorption, respectively. Reproduced with permission.<sup>44</sup> Copyright 2020, Wiley-VCH.

(E) The left part is components composited of the RIG and their structures, and the right part is a schematic of the moisture sorption and evaporation for the RIG.

(F) The hygroscopic kinetics of RIG at different RHs. Reproduced with permission.<sup>45</sup> Copyright 2021, Wiley-VCH.

liquid-holding and swellable abilities, achieving a self-supported solid form for liquid sorbents storage. Accordingly, there is a great interest in the preparation of MPGs with liquid sorbents within the polymer networks for moisture sorption, which is generally achieved through solvent displacement and *in situ* copolymerization.

For example, through direct immersion in concentrated solutions, LiBr, CaCl<sub>2</sub>, and ZnCl<sub>2</sub> aqueous solutions could be encapsulated in well-designed polymer networks to obtain various MPGs,<sup>71,73,74</sup> which usually exhibited a passive hygroscopicity and could spontaneously regenerate through moisture sorption after dehydration. As shown in Figures 6A and 6B, inspired by the structure and function of *Tillandsia* leaves, our group has reported a hygroscopic organogel (POG) whose hydrophilic polymer networks are designed to accommodate hygroscopic glycerol liquid for moisture uptake through a facile solvent displacement.<sup>44</sup> Moreover, 2D Raman mapping was investigated to track the sorption path of water molecules during moisture uptake. From the results, it could be observed that water molecules were captured by the surface of POG and then further diffused into its interior driven by the same osmotic effect as that of liquid sorbents (Figure 6C). Therefore, the POG could take advantage of sustainable moisture sorption of glycerol liquid and swellable features of polymeric networks, thus contributing to a high ESC. As a result, such an integrated POG showed a superhigh equilibrium



moisture sorption of  $16.01 \text{ kg m}^{-2}$  under 90% RH for 84 h coupled with significant swelling (Figure 6D).

Ionic liquids are versatile hygroscopic liquids that can provide a higher hygroscopicity and more reliable physical/chemical stability than other common liquid sorbents.<sup>78,81</sup> More recently, we also proposed an atmospheric hygroscopic ionogel (RIG) by *in situ* copolymerization, in which a highly hygroscopic ionic liquid of 1-ethyl-3-methylimidazolium Ac was accommodated into a hydrophilic poly(acrylic acid-co-2-acrylamido-2-methylpropane sulfonic acid) network for moisture uptake<sup>45</sup> (Figure 6E). As a result, a fast and high-capacity moisture uptake of 0.96, 0.50, and  $0.24 \text{ g g}^{-1}$  for 12 h at RHs of 90%, 70%, and 50%, respectively, was achieved by the RIG, which was competitive with other reported state-of-the-art sorbent materials<sup>41,78,80,82</sup> (Figure 6F).

### PROMISING APPLICATIONS OF HPGs

As previously discussed, HPGs can realize spontaneous AMH from the air, therefore exhibiting a great promise in sustainable water and energy applications. Moreover, owing to their highly tunable structures and functions, HPGs have functioned as appealing materials for realizing efficient AME by taking advantage of captured moisture. In this section, the state-of-art demonstrated water and energy applications of HPGs for AME, including energy management and freshwater generation, are firstly introduced and discussed. Moreover, we also summarize the essential information of cutting-edge AME technologies with their desirable HPG properties in Table 2.

#### Energy management

Owing to their declining and non-renewable reserves, traditional ways of energy generation from fossil fuels seem to be limited in a near future. Therefore, reasonable energy management, including energy harvest, efficiency promotion, and energy thrift, is what people have been striving for, particularly in this energy-consuming society. Given its ubiquitous and sustainable features, atmospheric moisture provides an alternative and promising resource for energy management, especially in remote areas without accessible liquid water sources. This field is acquiring increasing attention, and recently much progress has been achieved in various forms of energy management based on HPGs, such as fuels production, thermal dissipation, electric generation, and hydrochromism.

#### Fuel production

Clean chemical fuels, such as hydrogen and oxygen gases, can be obtained from water through water-splitting technologies. Unlike traditional water-splitting systems that require regular water replenishment, atmospheric water splitting (AWS) can spontaneously uptake moisture from the air and achieve water enrichment for subsequent water splitting, thus gaining tremendous attention.<sup>18</sup> Owing to abundant bond sites, active materials can be easily and stably incorporated into HPGs for durable catalysis. Moreover, high surface area and rich porous structures in the HPGs ensure an improved mass and charge transport and are also prone to provide more chances for reactants to contact with catalysts. Moreover, all complicated components in AWS systems can be efficiently integrated into HPGs to take full advantage of gelation chemistry. In this respect, HPGs exhibit great potential to serve as ideal candidates for AWS.<sup>6</sup>

In a typical AWS system, a piece of HPG usually serves as the electrolyte and is sandwiched between two electrodes; moreover, suitable catalysts are selected to be

**Table 2. Summary of various cutting-edge AME technology-based HPGs for energy management and freshwater generation**

AME technology	Desired HPG properties	Driving sources	Products
<b>Energy management</b>			
fuels production <sup>34,59,60,83</sup>	1. high moisture uptake 2. efficient combination of catalysts 3. high mass and charge transport	sunlight, electricity	hydrogen, oxygen
thermal dissipation <sup>45,73–75</sup>	1. high moisture uptake 2. high heat conduction and IR emission 3. high structural stability	waste heat	efficiency improvement
electric generation <sup>84–87</sup>	1. high moisture uptake 2. chemical structure gradient 3. open mesopores structure and charged pore surface	ion gradient or continuous water flow	electricity
hygrochromism <sup>47</sup>	1. high moisture uptake 2. nanoporous structure	sunlight or electricity	energy saving
<b>Freshwater generation</b>			
freshwater collection <sup>30,31,36,38–44,53,71,88</sup>	1. high moisture uptake 2. easy regeneration 3. fast sorption/desorption kinetics	thermal energy	freshwater
modern agriculture irrigation <sup>72</sup>	1. high moisture uptake 2. excellent water retention	thermal energy	agriculture irrigation

incorporated into it for captured water splitting. In this field, Tan's group has developed a series of seminal works on HPGs-based AWS for the generation of chemical fuels.<sup>59,60,83</sup> They have established an integrated AWS apparatus based on various water splitting systems, including electrolysis,<sup>60</sup> photoelectrochemical cell,<sup>60,83</sup> and photocatalysis.<sup>59</sup> A recent study introduced a hybrid catalyst in which 2D MoS<sub>2</sub> nanosheets interfaced with ferroelectric BaTiO<sub>3</sub> (BTO) were introduced into a Co-based HPG to decompose absorbed water for hydrogen and oxygen generation<sup>83</sup> (Figure 7A). As shown in Figure 7B, Co-based HPG can supply plenty of water sources via moisture sorption for splitting (2.5 g g<sup>-1</sup>, 0.0167 g cm<sup>-2</sup> for 24 h), and the solar cell can offer an electric bias to drive the catalysis process. Moreover, the MoS<sub>2</sub>/BTO catalyst is capable of breaking down absorbed water with an enhanced effect due to improved transfer of electrons and ions. As a result, this AWS device could generate ~1.78 mmol of H<sub>2</sub> and ~0.82 mmol of O<sub>2</sub> in 10 h powered with a solar cell, and the corresponding conversion efficiency of current to oxygen is greater than 90%.

In another work, Tan's group further developed an artificial photocatalysis system for AWS.<sup>59</sup> In brief, they chose a photocatalyst of Cu<sub>2</sub>O@BaTiO<sub>3</sub> as a water digester and evenly dispersed it into HPGs for photo splitting of absorbed water (Figure 7C). The photogenerated electron and hole could efficiently migrate to (100) and (111) planes of Cu<sub>2</sub>O for water breakdown, driven by the crystal planes' electric field in the Cu<sub>2</sub>O and the built-in electric field of BaTiO<sub>3</sub>. Moreover, hygroscopic Co- and Zn-based HPGs were both prepared in this system to act as water harvest machines for the above artificial photocatalysis system (Figure 7D). As a result, the Co-based HPG presented a more superb hygroscopic capability and larger water splitting amounts than those of the Zn one, achieving 450 and 59.6 mg for 24 h, respectively, under 85% RH (Figure 7E). Furthermore, the photo splitting capacities of resulted AWS devices were also measured under LED irradiation. Eventually, the AWS system with Co-based HPG also showed higher photocurrents than that of the Zn-based one both in water reduction and oxidation (Figures 7F and 7G). At this point, the amount of absorbed water from the air was identified as the key to water splitting, the higher it is the better it will be for water splitting.

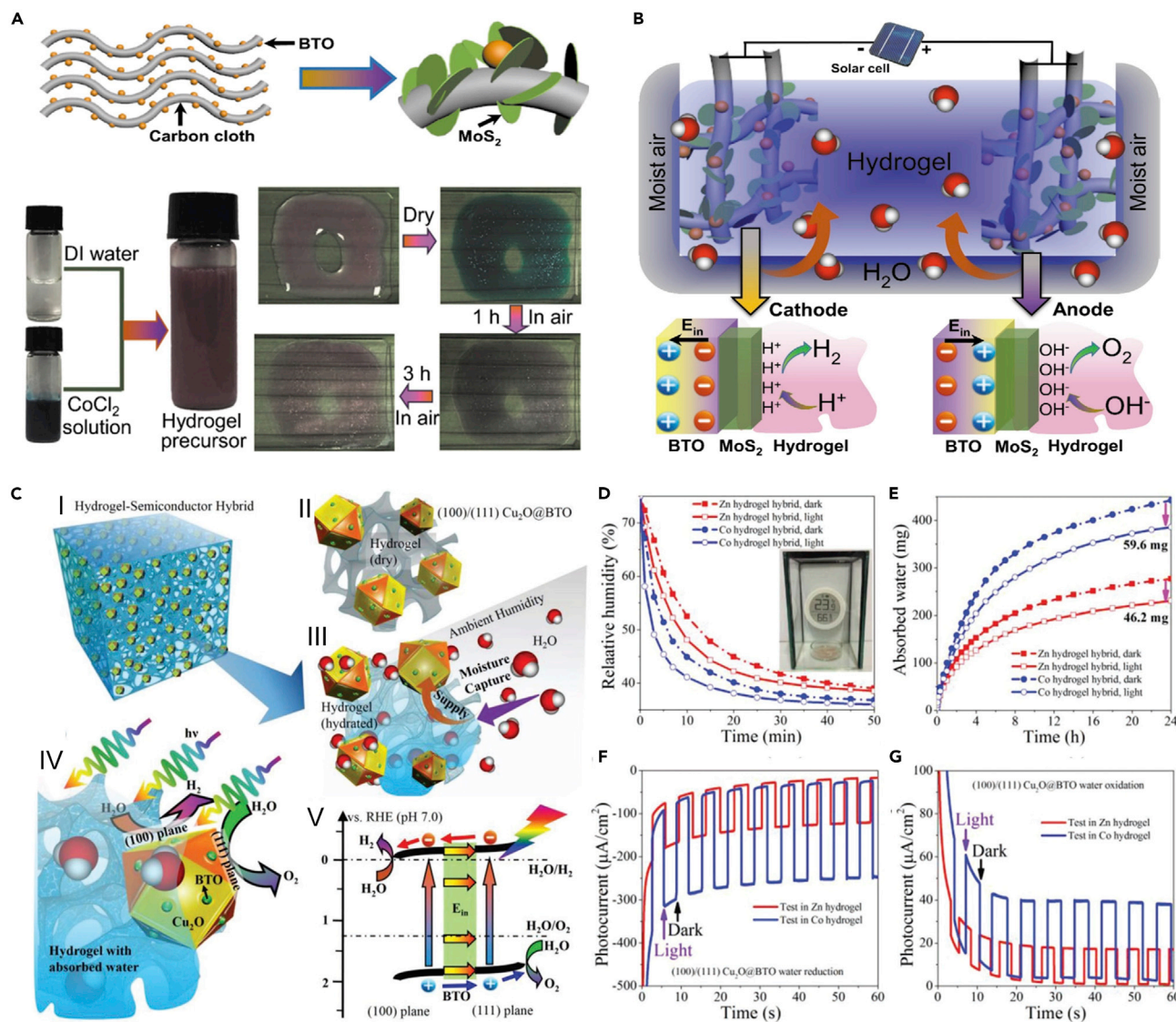


**Figure 7. Examples of HPGs for fuels production**

(A) Schematic of the Co-based HPG synthesis process.

(B) Schematic of the mechanism of AWS based on a Co-based HPG. Reproduced with permission.<sup>83</sup> Copyright 2020, Wiley-VCH.

(C) Schematic of the AWS process for (100)/(111)  $\text{Cu}_2\text{O}@\text{BTO}$  hybrid HPGs.

(D) The dehumidification curves of two HPGs hybrids in a sealed environment.

(E) Moisture uptake of two HPGs hybrids at 85% RH for 24 h.

(F) Water reduction at 0 V versus RHE for two HPGs hybrids under LED illumination.

(G) Water oxidation at 1.23 V versus RHE for two HPGs hybrids under LED illumination. Reproduced with permission.<sup>59</sup> Copyright 2019, Wiley-VCH.

Despite the encouraging progress in HPGs-based AWS, more efforts still need to be devoted to further improving their energy conversion efficiency. Currently, the energy conversion efficiencies of these AWS systems are still very low, especially compared with mature aqueous splitting ones, so they need to be further improved. In this regard, introducing more high-active catalysts into HPGs is a crucial direction for future research, in which their uniform dispersion in the gel networks should be also considered. Moreover, the enhanced mass and charge transport through corresponding gel network designs in HPGs can further promote their AWS efficiency. Furthermore, the quantitative optimization of hygroscopic amounts of HPGs also

facilitates enhanced AWS performances. In addition, there are challenges in the separation and storage of gases obtained from AWS that deserve our attention.

### *Thermal dissipation*

As known, thermal dissipation plays an essential role in the efficient and stable working of electronics. Generally, electronic devices will have a heat accumulation during their operation, resulting in significant performance degradation, and hence require cooling equipment to dissipate excessive waste heat.<sup>89</sup> Due to its large latent heat ( $\sim 2,400 \text{ kJ kg}^{-1}$ ), water desorption has been considered to be a hopeful alternative for heat removal without extra energy input.<sup>29,90</sup> Since HPGs can be regenerated through spontaneous moisture sorption after their inner water evaporates, it is highly anticipated that they may serve as self-sustained evaporative cooling materials for the thermal management of electronics. In this regard, the moisture uptake of HPGs is the most critical factor that decides their cooling performance, in which more captured moisture by HPGs can facilitate more thermal dissipation through evaporation. Recently, many impressive works have laid a solid foundation for further research.<sup>29,45,71,73,75,90</sup> For example, Pu et al. have demonstrated a polyacrylamide (PAAm) hydrogel containing considerable  $\text{Li}^+$  and  $\text{Br}^-$  ions, which could efficiently lower the temperature of a working solar cell to improve the corresponding efficiency through evaporative cooling, and was able to capture moisture in the air to regenerate itself in dormancy<sup>73</sup> (Figure 8A). There was a temperature drop of  $\sim 13^\circ\text{C}$  when the resulted hydrogel was attached to the photovoltaic (PV) cell under one sun illumination. Therefore, the solar-to-energy efficiency also increased to 15.5% from 14.5% of the natural cooling one. It is worth noting that the dehydrated hydrogel could regenerate to its initial state at night without any external energy input, ensuring its practicality and sustainability. Similarly, this hydrogel was also employed to cool down a cell phone chip that generates tremendous undesired heat triggered by high-power consumption (Figure 8B). Compared with natural cooling, the operation temperature of the chip had a noticeable decline of  $15.2^\circ\text{C}$  as the hydrogel was applied to its surface (Figure 8C). Moreover, the power of the chip was correspondingly improved with decreasing operation temperature, which facilitated supporting the chip to implement more functions, particularly in the coming fifth-generation mobile network.

Despite the rapid development of evaporative cooling based on HPGs, this remains a considerable challenge. For example, significant mechanical deformations caused by excessive water evaporation of HPGs probably cause their interfaces to be unreliable and even cool performance degeneration.<sup>73,90</sup> Therefore, appropriate strategies should be considered to solve this unstable interface between the thermal surface and HPGs. We recently developed a hygroscopic ionogel (RIG) composed of a hydrophilic polymeric skeleton and a hygroscopic ionic liquid medium to achieve an efficient and durable self-sustained evaporative cooling for thermoelectric performance enhancement of the TEG<sup>45</sup> (Figure 8D). Of note, the introduction of rGO can effectively increase the heat conduction of RIG, which can realize stronger thermal conduction for faster thermal dissipation. Most importantly, the presence of ionic liquid enabled the RIG to have not only an intensive hygroscopicity but a considerable adhesive property, leading to a dynamically stable cooling interface assisted by supramolecular adhesions for durable evaporative cooling (Figure 8E).

Furthermore, HPGs also have been applied to the thermal self-protection of batteries for working safety. Recently, Yang et al. demonstrated using zinc chloride-enriched hydrogel electrolytes (Zn-PAAm hydrogel) to achieve efficient thermal self-protection of zinc-ion batteries.<sup>74</sup> As illustrated in Figure 8F, a significant amount



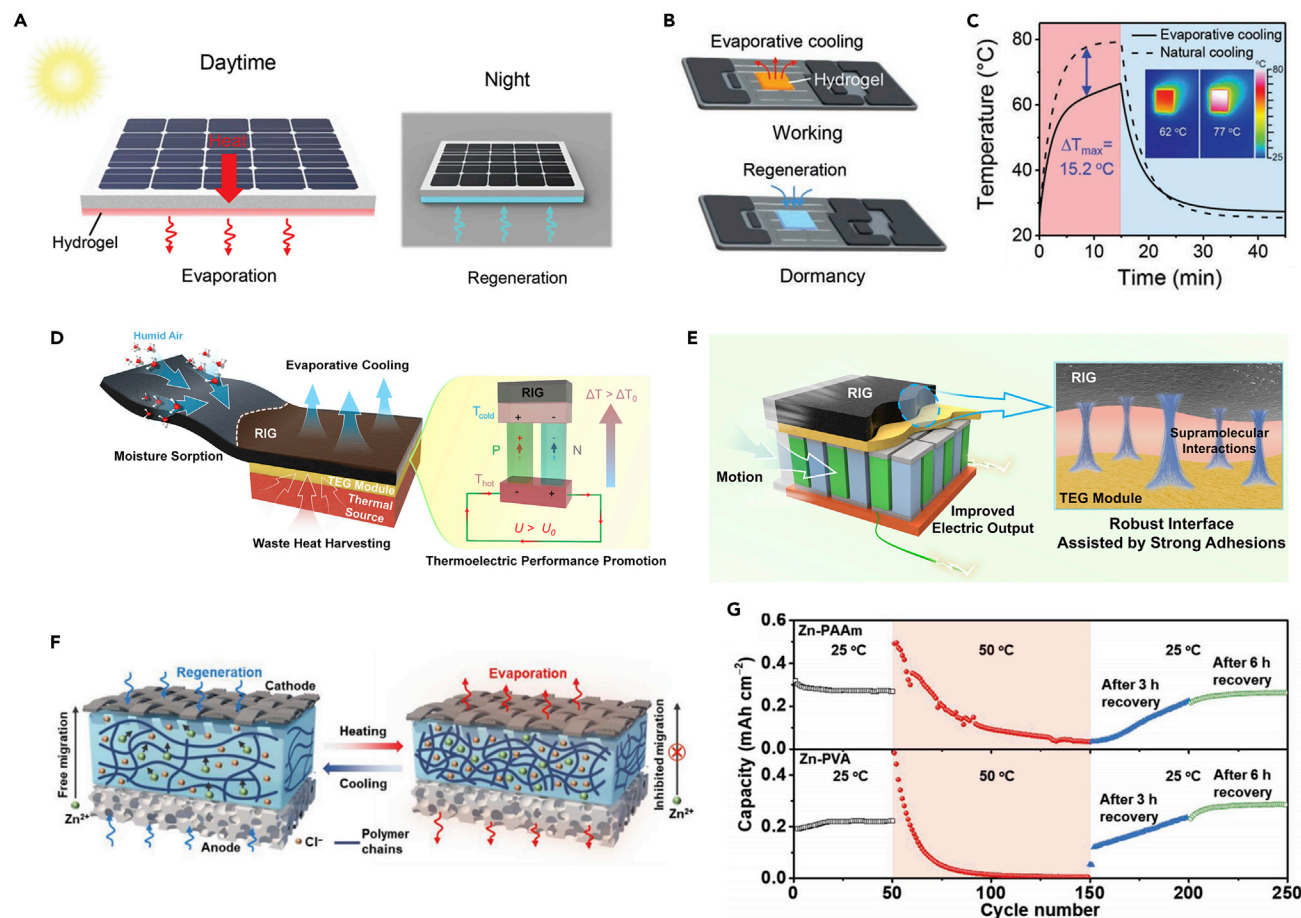


**Figure 8. Examples of HPGs for thermal dissipation**

- (A) The evaporative cooling for solar cells enabled by a hygroscopic LiBr-contained PAAm hydrogel.  
 (B) Schematic illustration of evaporative cooling for the phone chip.  
 (C) The temperature changes of the chip with and without evaporative cooling. The left inset is the IR image of the chip with evaporative cooling, and the right one refers to IR images of the chip without evaporative cooling. Reproduced with permission.<sup>73</sup> Copyright 2020, Wiley-VCH.  
 (D) The hydroscopic RIG was applied to cool down the cold side of TEG to enlarge its temperature gap across the whole device for its thermoelectric performance enhancement through self-sustained evaporative cooling.  
 (E) The RIG can realize a robust cooling interface owing to its strong adhesions, contributing to a stable and durable evaporative cooling both in static and moving states. Reproduced with permission.<sup>45</sup> Copyright 2021, Wiley-VCH.  
 (F) The working principle of self-protective zinc-ion batteries with hydroscopic hydrogel electrolytes.  
 (G) The demonstration of thermal self-protection of the zinc-ion battery. (F and G) Reproduced with permission.<sup>74</sup> Copyright 2020, Wiley-VCH.

of water inside a Zn-PAAm hydrogel could evaporate to dissipate heat generated by fast charging/discharging of batteries, thus relieving the local high temperature. Meanwhile, the migration of ions in the hydrogel electrolyte would be limited and eventually wholly interrupted as the number of water ions declines. This inhibited behavior of electrolyte ions would cut off the working of the batteries to prevent a fire caused by excessive local temperature. In addition, owing to its hygroscopicity, the dehydrated electrolyte could regenerate into its initial state through moisture sorption from the air in the cooling period. As a result, the resulting hydrogel electrolyte performed efficient thermal self-protection for the zinc-ion batteries (Figure 8G). The battery with the Zn-PAAm hydrogel electrolyte immediately activated self-protection mode to shut off the capacity output once it was placed in a hot temperature environment. When it cooled down, the battery could recover to its original state in 3 h. Note that this thermal self-protection strategy was also suitable for PVA,



a common electrolyte, which demonstrated similar results with the Zn-PAAm electrolyte.

Notably, the thermal-management properties of HPGs, such as heat conduction and infrared (IR) emission, can play critical roles during thermal dissipation and should be also highly considered in follow-up research, which will further promote their cooling capabilities via extra thermal radiation and thermal convection.

### *Electric generation*

The process of moisture sorption can directly be exploited to induce an electric generation, that is, moisture-enabled electricity generation (MEG), which originates from the interactions between water molecules and solid surfaces.<sup>91</sup> Benefiting from their high hygroscopicity, abundant porous structures, as well as plentiful hydrophilic functional groups, HPGs are regarded as one of the emerging materials for MEG. It is worth noting that there have been two primary mechanisms to explain MEG, namely, gradient diffusion and streaming current.

Generally, gradient-diffusion MEG is achieved by creating the chemical structure gradient in HPGs. In this case, the electricity is generated from ion or proton migration behaviors triggered by reactions between water molecules and hydrophilicity-gradient surfaces. For instance, Qu's group has proposed a hygroscopic anion-ion-gradient polypyrrole aerogel (g-3D-PPy) for vapor-activated electric generation<sup>84</sup> (Figure 9A). The detailed mechanisms of electric generation of g-3D-PPy are shown schematically in Figure 9B. With the increased concentration of captured water in g-3D-PPy, the solvation effect will dissociate the  $\text{Li}^+$ - $\text{ClO}_4^-$  bond to release removable  $\text{Li}^+$  and confine  $\text{ClO}_4^-$  ions with PPy chains. Afterward, a  $\text{Li}^+$  concentration difference will spontaneously form across the whole device due to an inherent gradient of  $\text{ClO}_4^-$  in g-3D-PPy, ultimately inducing an output of electricity. Conversely, a reverse current is also generated owing to recombination between  $\text{Li}^+$  ions and  $\text{ClO}_4^-$  after water desorption.

Beyond ions, proton liberation activities in the HPG induced by interactions between hydrophilic groups and water are also used to generate electricity. He et al. recently fabricated a moisture sorption composite hydrogel (TCGP) for MEG by dispersing tannic acid-CNTs into PVA gel<sup>85</sup> (Figure 9C). As shown in Figure 9D, the absorbed water molecules can protonate PVA molecules to set free protons, which will diffuse to produce a proton concentration gradient for electricity output. As a result, the voltage generated by TCGP rapidly increases up to 80 mV when exposed to it in a moist environment for 16 s (Figure 9E).

Similarly, a MEG device consisting of gelatin molecules has been reported by Mandal et al., whose power generation is also ascribed to the production and transferring of protons<sup>86</sup> (Figure 9F). We can observe that the electric output performances can be significantly improved using an asymmetric electrode design, in which the corresponding short circuit current density ( $J_{\text{SC}}$ ) and open-circuit voltage ( $V_{\text{OC}}$ ) are  $7.77 \mu\text{A cm}^{-2}$  and 0.71 V at 90% RH, respectively (Figures 9G and 9H).

However, the above MEG devices only provide an instantaneous power generation owing to the fading of the resulted ions gradient, thus restricting themselves in some practical applications. The streaming current derives from a water flow along a charged surface in a solid channel.<sup>92</sup> Therefore, a common strategy for streaming current is to construct an open mesoporous structure and a charged pore surface in HPGs. Recently, Li et al. have realized a stable streaming potential by exposing

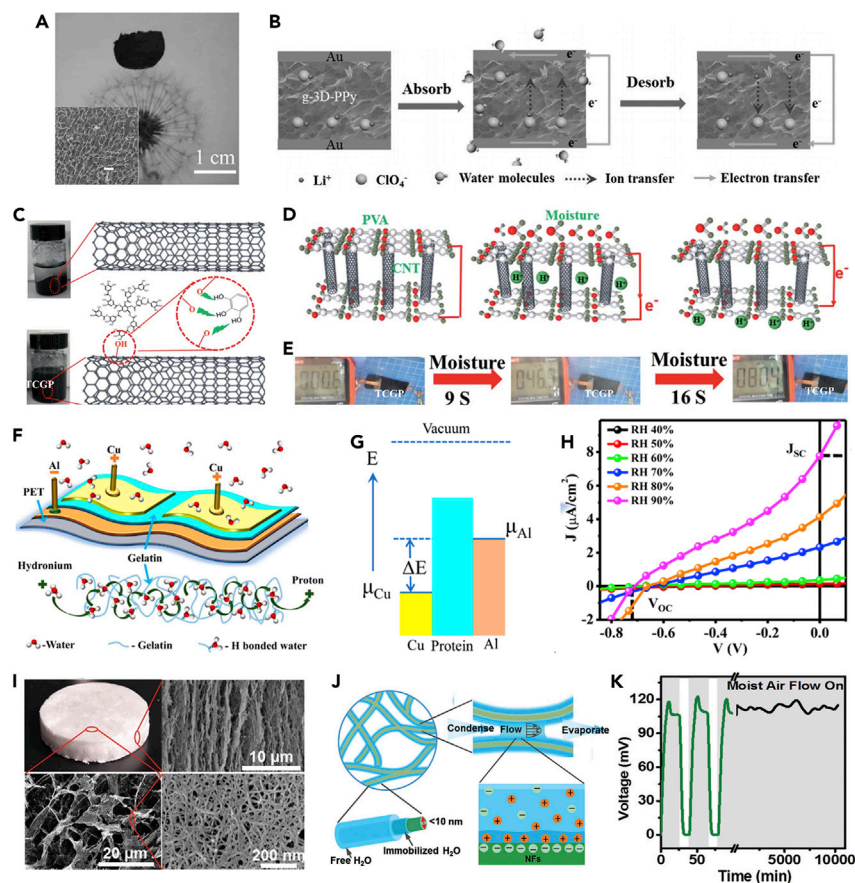


**Figure 9. Examples of HPGs for electric generation**

(A) Photo of 3D PPy hydroscopic aerogel.

(B) The working mechanism of 3D PPy aerogel for MEG. Reproduced with permission.<sup>84</sup> Copyright 2016, Wiley-VCH.

(C) Illustration of TCGP and its compositions.

(D) The mechanisms of electric generation of the TCGP hydrogel.

(E) The demonstration of the power generation process. Reproduced with permission.<sup>85</sup> Copyright 2020, Royal Society of Chemistry.

(F) Schematic design of MEG devices based on hygroscopic gelatin.

(G) Schematic showing the work function difference of asymmetric electrode design.

(H) The *I*-*V* curves of the device at different RHs. (F-H) Reproduced with permission from.<sup>86</sup> Copyright 2020, American Chemical Society.

(I) Optical and SEM images of freeze-dried TEMPO-CNFs aerogel.

(J) Schematic of the electric generation of TEMPO-CNFs aerogel.

(K) The  $V_{oc}$  changes while switching moist airflow on (gray) and off (white). Reproduced with permission.<sup>87</sup> Copyright 2019, Wiley-VCH.

biological hygroscopic TEMPO-cellulose nanofibrils (TEMPO-CNFs) aerogels in the moist airflow<sup>87</sup> (Figure 9I). The TEMPO-CNF aerogel could easily take up water molecules in the humid air flow owing to sufficient hydrophilic groups on their surface, liquefy them in their mesopores by capillary condensation, and eventually form them into water streams driven by water evaporation. This water flow on the charged surface of the TEMPO-CNFs would induce an electronic double layer and produce a streaming potential (Figure 9J). Accordingly, the TEMPO-CNFs could trap moisture when exposed to a humid airflow, and produce considerable electric output at RHs varying from 55% to 99%. Note that the corresponding voltage of TEMPO-CNFs would drop down to zero as the airflow cut off, and could return to the equilibrium

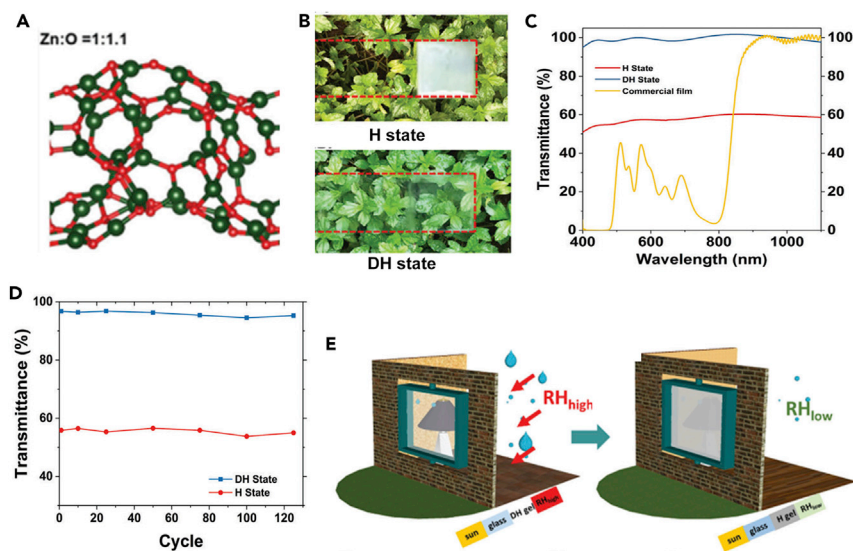


**Figure 10. Examples of HPGs for hydrochromism**

- (A) Simulated structure of the MSG with Zn:O ratios of 1: 1.1.  
(B) Optical images of the MSG in hydrated (H) state (top) and dehydrated (DH) state (below).  
(C) Optical transmittance of the MSG in H and DH states.  
(D) Optical transmittance of the MSG between H and DH states in a cyclic experiment.  
(E) Schematic of a hydrochromic window based on optical transmittance changes of the MSG triggered by humidity. Reproduced with permission.<sup>47</sup> Copyright 2018, Royal Society of Chemistry.

value in  $\sim 20$  min when the airflow was turned on again and remained stable for up to 10,000 min (Figure 9K).

### Hydrochromisms

Moisture can stimulate optical property changes of polymer gels, which has been extended to the applications of smart windows for energy savings in buildings. For example, Nandakumar et al. creatively reported a moisture-scavenging gel (MSG) with nanoporous structures that can achieve switching of optical property under stimulation of moisture<sup>47</sup> (Figures 10A and 10B). A liquid-air interface would be created in the porous structures of MSG after moisture sorption, which enhances the scattering of incident lights, resulting in a drastic drop in light transmission both in visible and IR light regions (Figure 10C). Moreover, the transmittance of MSG returned to 100% when water was completely desorbed, and the above processes were reversible without any decline in 125 cycles (Figure 10D). As a proof-of-concept, this MSG was coated on the window to regulate indoor humidity and temperature (Figure 10E). The hygroscopicity of MSG could enable indoor humidity below the triggering boundary of discomforts, and its opaque states after moisture sorption would also hinder sunlight and prevent the indoor temperature from rising. Such an MSG with unique moisture-responsive chromatic and humidity regulation properties is energy friendly and promising to significantly reduce the energy consumption of buildings in the future.

### Freshwater generation

Freshwater shortage is still one of the most rigorous challenges in this era, and urgently remains to be solved.<sup>93–95</sup> In past decades, great efforts have been made to convert seawater or wastewater into freshwater by various freshwater production technologies, such as filtration,<sup>96–99</sup> reverse osmosis,<sup>100</sup> membrane distillation,<sup>101,102</sup> and solar-driven purification.<sup>92,103–109</sup> These well-established methods, however, are only applicable in coastal cities with accessible water sources, but

require hard work in inland areas where liquid water is physically scarce. Owing to its ubiquitous features, a combined strategy of the sorption-based AWH strategy and subsequent extraction of water from the sorbents provides an alternative solution for freshwater generation in some remote inland and off-grid areas, demonstrating great promise in freshwater collection and agricultural irrigation.<sup>12,14,16,17,48</sup>

#### *Freshwater collection*

From the perspective of sustainability, a desirable AWH system requires a minimal energy input for freshwater production. In this sense, solar-driven evaporation and thermo-responsive phase separation are two suitable strategies for HPGs to realize energy-efficient water release after moisture sorption.

*Solar-driven atmospheric moisture collection.* Recently, solar-driven evaporation has become a promising alternative to drive water extraction from sorbents to harvest freshwater.<sup>6,27,94</sup> In this sense, HPGs are desirable material platforms for solar-driven atmospheric moisture collection (SAMC) due to their easy integrations with photothermal components, highly tuneable properties, and large-scalable fabrication. In this section, we look into impressive progress in freshwater collection by SAMC based on HPGs.

A typical SAMC device is illustrated in [Figure 11A](#), where the freshwater collection for hydrated HPGs is mainly composed of three processes: evaporation, condensation, and collection. To explain this process, a psychrometric chart was selected to describe the working cycle of water evaporation and condensation in the SAMC device<sup>48</sup> ([Figure 11B](#)). Specifically, the captured water molecules by HPGs can be firstly evaporated under solar irradiation in a sealed device, and thus the partial pressure in the devices simultaneously increases to saturation. After exchanging heat with the cold device wall, the water vapor condenses and liquefies into water droplets, slips down along the wall owing to gravity, and is eventually collected. Apparently, the final freshwater yield in such a system based on HPGs is determined by the following crucial factors: (1) desorption rates of HPGs; (2) condensation conditions; and (3) cyclic times of the sorption-desorption process in the required time ([Figure 11C](#)).

The water evaporation (i.e., desorption) of hydrated HPGs is the most essential issue in the SAMC for freshwater collection, heavily depending on their material designs; therefore, here we discuss it. More specifically, factors influencing the water evaporation of hydrated HPGs mainly include solar absorption, desorption area, and evaporation enthalpy of captured water. As discussed above, since the water evaporation in the SAMC is powered by thermal energy converted from solar energy, the high solar absorption of HPGs is actively needed for achieving desirable freshwater extraction. To date, various state-of-the-art solar absorbers, including plasmonic particles,<sup>110</sup> carbon nanomaterials,<sup>111</sup> and conjugated polymers,<sup>112</sup> were combined into HPGs to provide them with a considerable photothermal performance. Among these solar absorbers, carbon nanomaterials, such as CNTs and rGOs, are the most available photothermal candidates in HPGs owing to their low cost, large scalability, easy integrability, and excellent stability.<sup>31,36,71</sup> Typically, these carbon nanomaterials are incorporated into HPGs through *in situ* gelation of a mixed pre-solution, and thus their hydrophilicity is key to uniform dispersion<sup>31</sup> ([Figure 11D](#)). In addition, the construction of the interpenetrating network of conjugated PPy during the polymerization of HPGs was recently reported to realize high solar absorption<sup>42,44,72</sup> ([Figure 11E](#)). Other photothermal materials, such as plasmonic metal nanoparticles and semiconductors, also can be evenly embedded into HPGs to achieve efficient photo-to-thermal conversions; however, there are still challenges in the practical implantation in terms of cost, stability, toxicity, and fabrication.

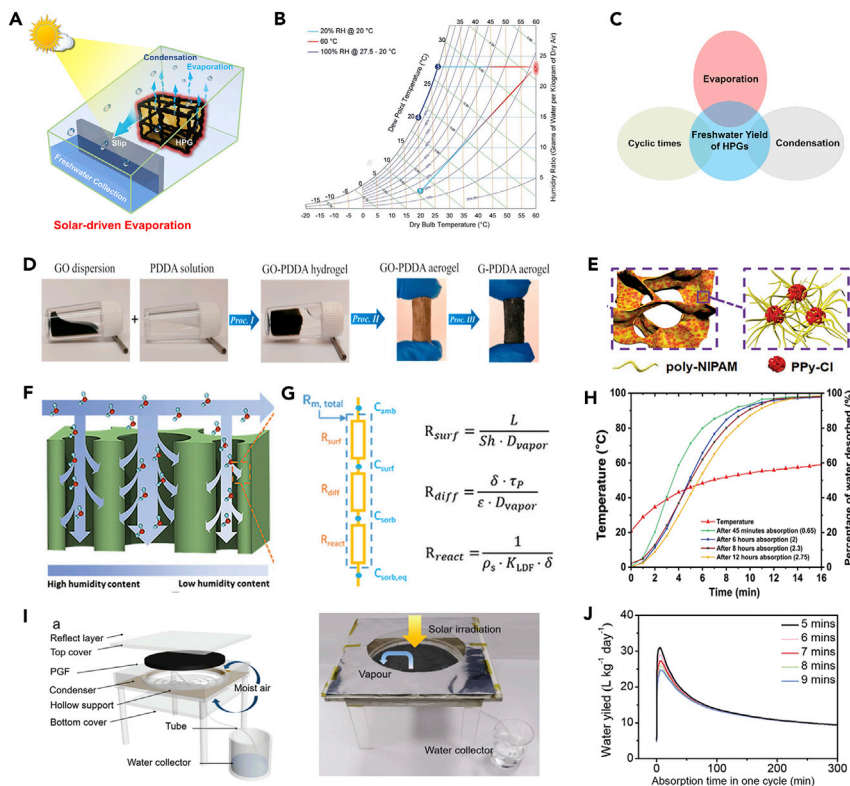


**Figure 11. Solar-driven atmospheric moisture collection of HPGs**

- (A) Schematic of a typical SAMC device.
- (B) Psychrometric chart between  $-20^{\circ}\text{C}$  and  $60^{\circ}\text{C}$ , demonstrating the processes of water evaporation and condensation in the SAMC device. Reproduced with permission.<sup>48</sup>
- (C) The factors affecting the freshwater yield of HPGs.
- (D) Schematic of the G-PDDA fabrication process, where rGOs acted as photothermal materials. Reproduced with permission.<sup>31</sup> Copyright 2020, Elsevier.
- (E) The photothermal PPy-Cl was interpenetrated with the poly-NIPAM networks for solar-to-thermal conversion. Reproduced with permission.<sup>42</sup> Copyright 2019, Wiley-VCH.
- (F) Schematic of moisture transport pathways from the air to the HPGs.
- (G) The mass transfer resistance analysis for moisture.
- (H) Desorption for HPGs with different absorption times as temperature increased. Reproduced with permission.<sup>32</sup> Copyright 2019, Wiley-VCH.
- (I) Schematic (left) and optical image (right) of the moisture harvester based on PGFs for multicyclic moisture sorption and desorption.
- (J) The predicted water yield per day by PGFs via an alternative sorption-desorption cycle. Reproduced with permission.<sup>30</sup> Copyright 2020, Wiley-VCH.

Apart from photothermal properties, the desorption area of HPGs is another crucial factor determining their water evaporation. In general, an enlarged desorption area realized by a porous structure or 3D structures in HPGs can contribute to promoting their water evaporation kinetics.<sup>30,31,39</sup> In addition, Xu et al. have proposed a mass transport resistance analysis for moisture transport in HPGs (Figures 11F and 11G), which demonstrated that the vertically aligned and hierarchical pores can further allow HPGs to improve desorption kinetics.<sup>39</sup>

Moreover, the evaporation enthalpy of captured moisture also plays an important role in thermal desorption. For adsorption-typed HPGs, most of their captured water is in the form of bound water, and thus weaker bond energy between the HPG surface and water molecules can achieve a lower evaporation enthalpy. In this regard,



physisorption of moisture has a lower evaporation enthalpy than that of chemisorption.<sup>14,32,47</sup> Based on this, Nandakumar et al. proposed a nanoporous hydrogel that could achieve a moisture concentration with the participation of physisorption, and thus demonstrated a low desorption temperature and rapid water desorption.<sup>32</sup> As a result, such a nanoporous hydrogel could desorb more than 98% of captured water within 13 min at below 55°C (Figure 11H). In addition, there is an obvious swelling for most HPGs after moisture absorption, in which the absorbed water can exist in many forms, such as free water, intermediate water, and bound water, owing to the regulation of polymer chains.<sup>113</sup> Specifically, the intermediate water is easier to release due to its lower enthalpy value, while the desorption of bound water highly depends on its bond energy with polymer chains. Therefore, it seems an available way to adjust the ratio of intermediate and bound water in hydrated HPGs to regulate their evaporation enthalpy in future research.

In addition to water evaporation of HPGs, an enhanced condensation is usually designed in SAMC for a higher freshwater yield. However, the condensation design is usually achieved by the integrated system design, such as thermal and photo management, for an enhanced vapor condensation to improve the desorption kinetics of HPGs. This strategy has become a general approach applicable to HPGs in practical applications. In this review, we mainly focus on the relationship between the intrinsic properties of HPGs and final freshwater generation, and thus this system-level condensation design will not be further discussed here. Very recently, Yang et al. and Ejeian and Wang have both presented comprehensive reviews on this important system-design strategy in SAMC for improved freshwater generation.<sup>16</sup>

Last, but not least, cyclic times of the sorption-desorption process in 1 day also affect the practical daily freshwater yield. Unlike traditional monocyclic ones, multicyclic atmospheric water harvesters based on HPGs have been developed for a higher freshwater production, which requires HPGs to have fast sorption and desorption kinetics.<sup>30,31</sup> As a proof-of-concept, Yao et al. demonstrated a multicyclic harvester using hygroscopic PGF with rapid sorption and desorption rates, in which PGF can achieve a rapid alternation between moisture sorption and desorption<sup>30</sup> (Figure 11I). According to theoretical predictions, the maximum freshwater yield of PGF would be over 31.2 L kg<sup>-1</sup> day<sup>-1</sup> experiencing cycles with 6-min moisture sorption, 5-min water desorption, and 2 min of cooling time (Figure 11J). In the outdoor experiment for 24 h, a considerable freshwater generation of 17.4 g g<sup>-1</sup> was achieved for PGF through a long cycle of 15 h sorption per desorption and 16 cycles of 25 min sorption per 5 min desorption, which was more than that of conventional monocyclic way.

*Thermo-responsive atmospheric moisture collection.* The thermo-responsive atmospheric moisture collection (TAMC) is achieved via the integration of thermo-responsive phase-transition polymers in HPGs. The unique thermos-responsive behavior of polymers, such as poly(*N*-isopropyl acrylamide) (PNIPAM), can allow them to undergo a huge volume change when their temperature slightly changes, allowing the separation of trapped moisture for freshwater collection just upon low-temperature heating.<sup>42,43,88</sup>

As shown in Figure 12A, once the temperature exceeds their critical solution temperature (LCST) of 32°C, the PNIPAM-based HPGs can rapidly change their hydrophilic/hydrophobic property and cause a drastic volumetric shrinkage to squeeze out most of the inner water. With this, Matsumoto et al. demonstrated a TAMC application of an interpenetrating polymer network (IPN) gel composed of a thermo-responsive PNIPAM polymer and hydrophilic sodium alginate networks<sup>88</sup> (Figure 12B). The

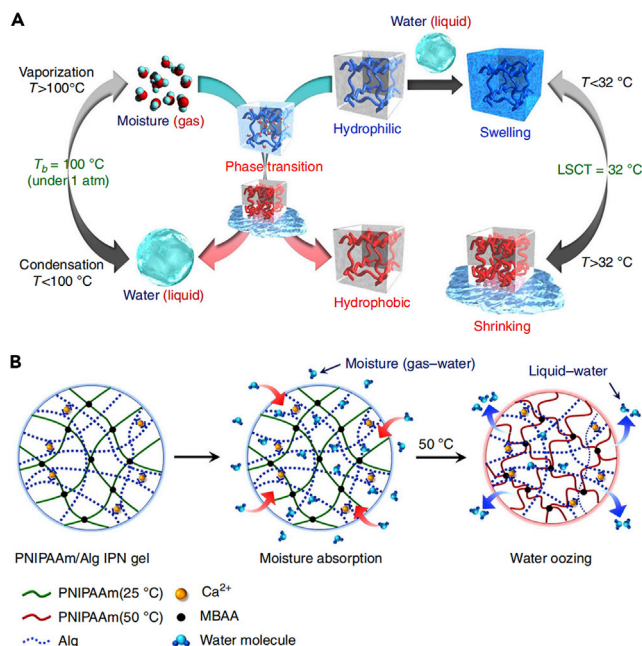


**Figure 12. Thermo-responsive atmospheric moisture collection of HPGs**

(A) The working principle of thermo-responsive phase-transition polymer gel.

(B) The moisture sorption and water oozing behaviors of IPN gel are triggered by temperature changes.

IPN gel could capture gaseous water from the air below its LCST and effectively release it in the form of liquid water when the temperature increases to  $50^\circ\text{C}$ . Therefore, the above concept of water collection realized by phase transition of polymer can provide an effective pathway to release the captured water of HPGs at low energy consumption.

Furthermore, Yu's groups developed a photothermal hygroscopic thermo-responsive HPG (SMAG) fabricated by interpenetrating PPy-Cl into a poly-NIPAM hydrogel, which can directly convert the solar energy into thermal energy to drive the thermo-responsive phase transition of poly-NIPAM.<sup>42</sup> As shown in Figure 13A, the SMAG has two modes of water desorption; that is, thermal-responsive shrink deswelling (express mode) and photothermal evaporation (normal mode). Therefore, SMAGs with different hydration contents both exhibited fast water release via express mode under solar irradiation (Figure 13B). Moreover, the residual water of SMAGs after rapid water extrusions can be also harvested through a traditional evaporation-condensation process (Figure 13C).

In another report, Yilmaz et al. proposed a novel HPGs (PC-MOF) composed of MIL-101(Cr),  $\text{CaCl}_2$ , and PNIPAM polymer gel with an autonomous water seeping property for atmospheric water collection.<sup>43</sup> Owing to steric pressure and restricted expansion of PC-MOF, the adsorbed water would condense and seep out after sorption saturates (Figure 13D). Importantly, moisture sorption and water seepage can happen simultaneously for water harvest without common evaporators/condensers (Figure 13E). In addition, the PC-MOF with a cone array geometry was fabricated to speed up removal of condensed water droplets in practical applications (Figure 13F). As a result, the resulting device demonstrated a considerable water uptake of  $6.04\text{ g g}^{-1}$  through seepage at 90% RH where solar radiation is scarce.

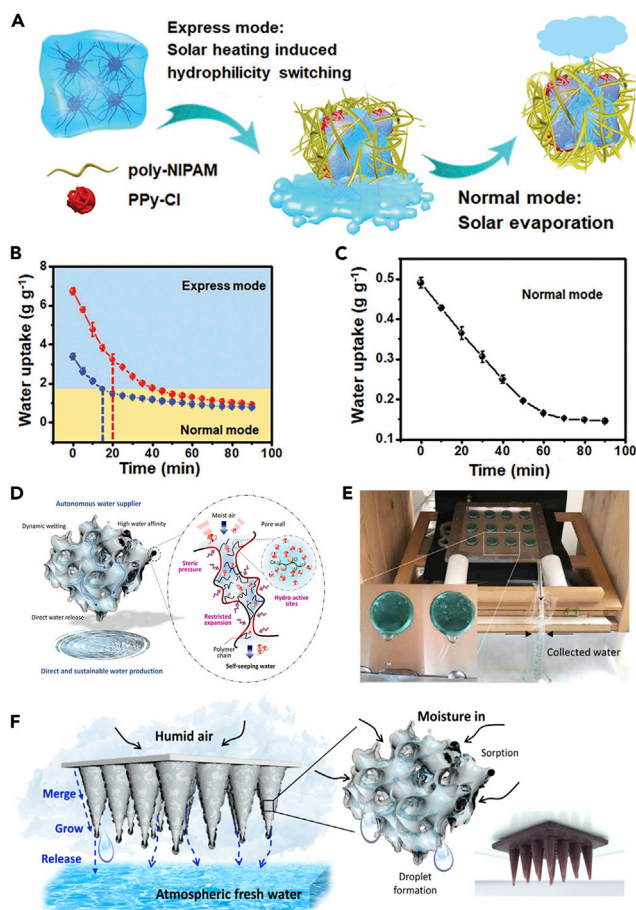


**Figure 13. Sustainable atmospheric moisture collection based on thermo-responsive HPGs**

(A) Schematic of water release of SMAGs under solar illumination.

(B) The water releasing curves of SMAGs with high water uptake.

(C) The water releasing curves of SMAGs with low water uptake. Reproduced with permission.<sup>42</sup>

Copyright 2019, Wiley-VCH.

(D) Schematic of the autonomous atmospheric water harvest based on PC-MOF.

(E) Optical image of atmospheric water harvest based on PC-MOF.

(F) The PC-MOF cone array for atmospheric water collection. Reproduced with permission.<sup>43</sup>

Copyright 2020, AAAS.

### Agriculture irrigation

The sustainable development of agriculture can ensure food security in the situation with explosive growth of the global population.<sup>114–116</sup> However, a huge demand for freshwater for agriculture irrigation casts a shadow on the sustainability of food. It is estimated that agriculture irrigation has accounted for more than 95% of total freshwater withdrawals in some developing countries.<sup>34</sup> As such, modern agriculture urgently needs to explore new technologies and renewable freshwater resources to meet the globally growing demand for food. As a huge and ubiquitous freshwater source, atmospheric moisture has a great promise for sustainably realizing agriculture irrigation.

Zhou et al.<sup>72</sup> have developed a conceptual atmospheric moisture irrigation system based on a hybrid hygroscopic material (SMAG-soil) composed of SMAG and soil. The SMAG-soil demonstrated working schematics of passive irrigation for plants and solar-driven environmental humidification in a sustainable way (Figure 14A).

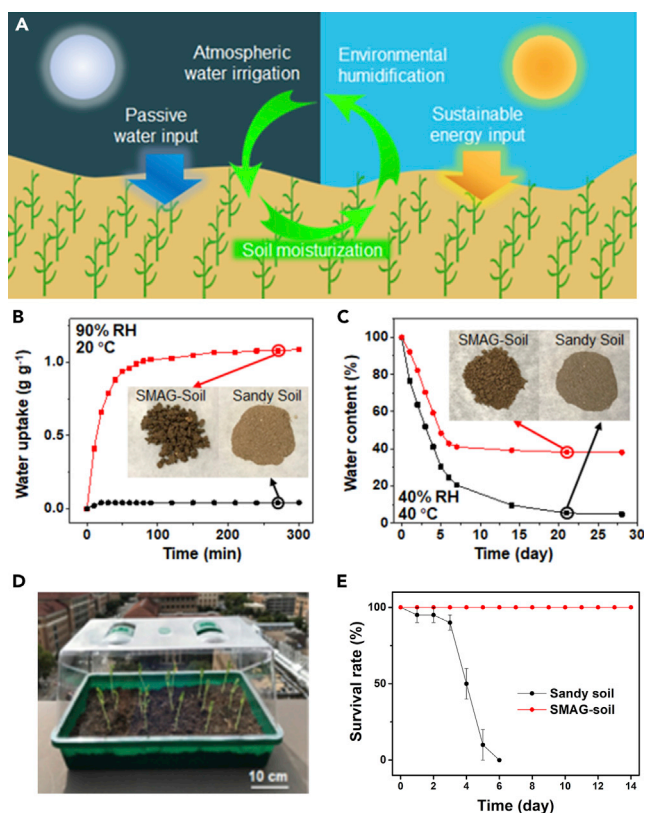


**Figure 14. Examples of HPGs for agricultural irrigation**

(A) The working schematic of SAMG-soil.

(B) The moisture uptake from the air at 90% RH and 20°C.

(C) The water-holding capability at 40% RH and 40°C.

(D) Optical image of outdoor atmospheric water irrigation.

(E) The survival rate of plants. Reproduced with permission.<sup>72</sup> Copyright 2020, American Chemical Society.

Significantly, the SAMG-soil demonstrated two orders higher moisture uptake than that of sandy soil, reaching up to  $1.1 \text{ g g}^{-1}$  (Figure 14B). Moreover, the SAMG-soil also presented a superb water-holding capacity. As shown in Figure 14C, the water content of sandy soil had a quick decrease of 80% within a week, but that of SAMG-soil could still maintain more than 40% after 4 weeks. Therefore, the SAMG-soil, with considerable moisture sorption property and water-holding ability, showed a promise for crop planting in environments without liquid water resources (Figure 14D). As a result, crops in the SAMG-soil demonstrated higher germination and survival rates than those in sandy soil (Figure 14E), indicating a great potential for sustainable agriculture in desertified regions.

More importantly, owing to their non-toxic, biodegradable, water-retaining characteristics, HPGs show promising potential to become preferable substrate materials to further replace common soils for plant growing in the future.

### Synergistic water-energy generators

At present, tremendous progress has been made in energy management and freshwater generation from moisture in the air. However, existing AME technologies are usually adopted separately and independently, which inevitably causes high costs and a huge waste. Allowing two or more functional units in an integrated system

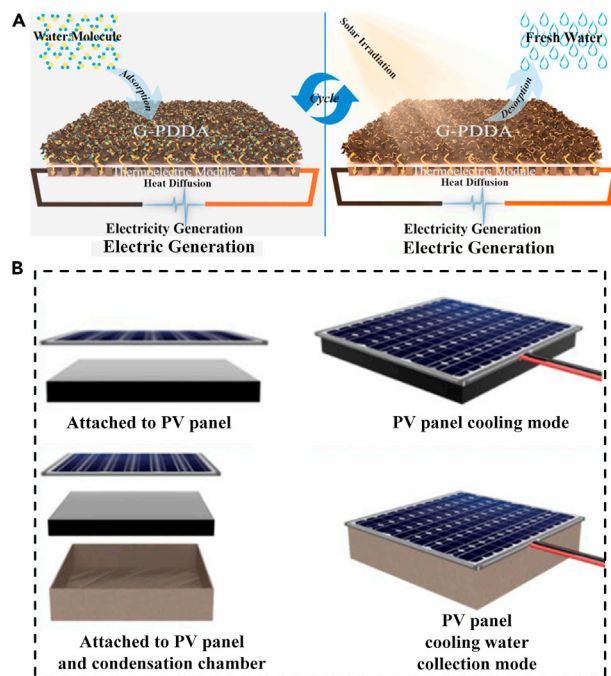


**Figure 15. Examples of HPGs for synergistic water-energy generators**

(A) Schematic of the simultaneous generation of electricity and freshwater by G-PDDA. Reproduced with permission.<sup>31</sup> Copyright 2020, Elsevier.

(B) Evaporative cooling for PV panels and freshwater collection. Reproduced with permission.<sup>71</sup> Copyright 2020, Springer Nature.

to simultaneously achieve energy management and freshwater generation in a mutually beneficial way has a great prospect for sustainable development.<sup>31,71,117–120</sup> More importantly, this field not only requires further development of HPGs to meet the desire for multifunctionality but needs further system-level design and optimization.<sup>121</sup> Therefore, more attention should be invested into inter-disciplinary research and close collaboration in different fields, such as material science, applied thermal engineering, and system engineering, to achieve more high-efficient synergistic generation.

In this regard, by combining hygroscopic photothermal HPGs with a thermoelectric module, Yang et al. have demonstrated a united water-electricity generation system<sup>31</sup> (Figure 15A). In this process, the heat generated by moisture absorption and solar absorption of HPGs caused the thermoelectric module to have an electric output, as well as freshwater being produced by HPGs through sorption and photo-thermal desorption.

In addition, Li et al. recently applied HPGs on a commercial PV panel to realize simultaneous evaporative cooling and freshwater collection<sup>71</sup> (Figure 15B). When HPGs were attached to the PV panel, the corresponding photo-to-electric efficiency of the PV panel significantly improved owing to its temperature lowering triggered by evaporative cooling of HPGs. Moreover, the water evaporated from HPGs could be effectively collected when the condensation chamber was employed. Notably, the dehydrated HPGs could easily regenerate to a hydrated state in the humid environment for the next operation, thus demonstrating a self-sustaining property.

## CONCLUSION AND PERSPECTIVE

Atmospheric moisture is a huge and ubiquitous water source but rarely noticed, which can provide a water supply without any geographical or/and hydrologic restrictions. Notably, HPGs outperformed many other sorption materials with unique advantages in AME technologies for energy management and freshwater generation. In this review, we discuss in detail most of the state-of-the-art progress of HPGs in moisture sorption mechanisms, material design and fabrication, and wide-ranging energy- and water-related AME applications.

Combined with the rational design of inherent physical/chemical structures or mixing hygroscopic components with polymeric networks, various well-designed HPGs have been developed. Furthermore, the easy integration of functional additives and the highly tuneable structures allow HPGs to further reutilize captured water for energy management and freshwater generation. Therefore, such an appealing HPGs-based system is regarded as one of the emerging material platforms for AME and demonstrates great promises in much cutting-edge energy- and water-related technologies (e.g., fuels production, thermal management, electric generation, hygromorphism, and freshwater collection, as well as agricultural irrigation).

Despite tremendous encouraging advances achieved in HPGs, there remain several challenges. For example, the limited amount of moisture sorption of HPGs restricts them from reaching maximum performance in following AME technologies. Therefore, it is highly desirable for HPGs to further improve their hygroscopic abilities, particularly in low RH regions. In this regard, according to the hygroscopic mechanism, strengthening their intrinsic affinity to water molecules and improving their water storage capability are two effective approaches to develop high-performance HPGs in the future. First, the introduction of more high-water-affinity species, such as inorganic ions ( $\text{Li}^+$ ,  $\text{Ca}^{2+}$ ,  $\text{Cl}^-$ ,  $\text{Ac}^-$ , etc.) and MOFs, into HPGs can significantly enhance their interactions with water molecules for higher hygroscopic performances in low RHs. Furthermore, the optimization of the swelling property of HPGs through molecular designs will significantly improve the water storage capability of HPGs, thus further promoting their moisture sorption. In addition, relatively low sorption/desorption kinetics also result in a low moisture uptake for HPGs on time-limited occasions. Approaches to increasing their specific surfaces via creating porous structures or 3D structures can effectively promote their kinetics for HPGs, which can derive from the enlargement of the air-solid interface. Moreover, especially for HPGs, the size of tested samples greatly influences their hygroscopic performance owing to their geometric macroscopic bulk. Therefore, a well-established characterization standard for evaluating the hygroscopic performances of HPGs should be proposed to identify their applicable applications and provide a reference for their further development. From the perspective of practical usage, an application-oriented evaluation system seems like a good method at this stage.

In terms of long-time operations, it is of great significance to improve the durability of HPGs. Remarkably, when exposed to polluted environments, the HPGs were usually designed to have a high affinity to gaseous impurities ( $\text{SO}_x$ ,  $\text{NO}_x$ ,  $\text{CO}_x$ , suspended particles, etc.) and further adsorbed them inside the polymer networks to get high-quality freshwater. However, the introduction of impurities onto sorption sites of HPGs may lead to a failure in moisture sorption. As such, concerns about removing or degradation of these pollutants for HPGs need to be considered to achieve their repeatability. Besides, structural changes that occur in the porous HPGs after sorption-desorption cycles also cannot be ignored, especially for organic



ones. Although their interconnected porous structure can be achieved through freeze drying, shrinkage or even collapse may happen in the incipient cycles of swelling and deswelling due to the capillary effect of these organic porous HPGs, which would result in declined hygroscopic performances in follow-up moisture sorption. In this regard, more research efforts should be invested to achieve the structural stability of porous gels to avoid these issues in their practical implementation.

Furthermore, the cost and production of HPGs are two basic aspects to be considered before they are brought into the market for mass application. Current material species for HPGs in AME technologies are relatively expensive and use unrenovable raw materials, which may increase the cost of energy and freshwater production, thus losing their competitive advantages with other technologies. Therefore, more low-cost and natural material systems should be developed to achieve HPGs with desirable cost and gain more appeal in the future. Moreover, the current reported technology of HPGs fabrication is primarily based on mold casting, which is considered to be conceptual, time consuming, and difficult to amplify for practical applications. In this regard, the emerging 3D printing and computational modeling technologies are expected to bring new insight into the mass production of HPGs.

In the AME process, if the water captured by HPGs cannot be fully utilized within the effective time, it will not only lead to limited product yield but result in incomplete regeneration of HPGs. Therefore, the full consumption of absorbed water of HPGs through materials and device optimization should be taken into consideration. Furthermore, exploring novel multifunctional HPGs for simultaneous energy and/or water multi-harvesting is also appealing in the AME. In this sense, although a few paradigms have appeared, an extensible combination of various existing energy- and water-related technologies are expected to achieve a mutually beneficial manner for HPGs in one sorption-desorption cycle through their rational designs. Moreover, rational system integration also significantly influences their practical application and remains very challenging. In other words, only current HPG materials integrated into advanced systems can realize their full potential to accelerate their marketization, so their further development requires inter-disciplinary research and close cooperation in different fields.

In the future, we believe that ideal HPGs for the AME should satisfy the following criteria: fast moisture sorption kinetics, high moisture ESC, easy regeneration, high durability, multiple integrated functions, low cost, and high commercial viability.

## ACKNOWLEDGMENTS

This work was supported by the Natural Science Foundation of China (52073295), the Ningbo Science and Technology Bureau (2021Z127), the Sino-German Mobility Program (M-0424), the Key Research Program of Frontier Sciences, the Chinese Academy of Sciences (QYZDB-SSW-SLH036), the Bureau of International Cooperation, Chinese Academy of Sciences (174433KYSB20170061), and the K.C. Wong Education Foundation (GJTD-2019-13).

## AUTHOR CONTRIBUTIONS

All authors contributed to writing the manuscript. T.C. directed the overall study.

## DECLARATION OF INTERESTS

The authors declare no competing interests.

## REFERENCES

1. Food and Agriculture Organization of the United Nations (2017). The Future of Food and Agriculture-Trends and Challenges (Food and Agriculture Organization of the United Nations).
2. Peter, B., Satoh, Y., Fischer, G., Taher Kahil, M., Scherzer, A., Tramberend, S., Fabiola Nava, L., Wada, Y., Eisner, S., Flörke, M., et al. (2014). Water Futures and Solution: Fast Track Initiative-Final Report (International Institute for Applied Systems Analysis).
3. Cosgrove, W.J., and Loucks, D.P. (2015). Water management: current and future challenges and research directions. *Water Resour. Res.* 51, 4823–4839. <https://doi.org/10.1002/2014wr016869>.
4. Halder, P.K., Paul, N., Joardder, M.U.H., and Sarker, M. (2015). Energy scarcity and potential of renewable energy in Bangladesh. *Renew. Sustain. Energy Rev.* 51, 1636–1649. <https://doi.org/10.1016/j.rser.2015.07.069>.
5. Anadon, L.D., Chan, G., Bin-Nun, A.Y., and Narayanamurti, V. (2016). The pressing energy innovation challenge of the US national laboratories. *Nat. Energy* 1, 16117. <https://doi.org/10.1038/nenergy.2016.117>.
6. Guo, Y., Bae, J., Fang, Z., Li, P., Zhao, F., and Yu, G. (2020). Hydrogels and hydrogel-derived materials for energy and water sustainability. *Chem. Rev.* 120, 7642–7707. <https://doi.org/10.1021/acs.chemrev.0c00345>.
7. Boretti, A., and Rosa, L. (2019). Reassessing the projections of the world water development report. *NPJ Clean Water* 2, 15. <https://doi.org/10.1038/s41545-019-0039-9>.
8. Mekonnen, M.M., and Hoekstra, A.Y. (2016). Four billion people facing severe water scarcity. *Sci. Adv.* 2, e1500323. <https://doi.org/10.1126/sciadv.1500323>.
9. Causes, Effects and Solutions to Global Energy Crisis, Conserve Energy Future, <https://www.conserve-energy-future.com/causes-and-solutions-to-the-global-energy-crisis.php>.
10. Li, Z., Xu, X., Sheng, X., Lin, P., Tang, J., Pan, L., Kaneti, Y.V., Yang, T., and Yamauchi, Y. (2021). Solar-powered sustainable water production: state-of-the-art technologies for sunlight-energy-water nexus. *ACS Nano* 15, 12535–12566. <https://doi.org/10.1021/acsnano.1c01590>.
11. Salehi, A.A., Ghannadi-Maragheh, M., Torab-Mostaedi, M., Torkaman, R., and Asadollahzadeh, M. (2020). A review on the water-energy nexus for drinking water production from humid air. *Renew. Sustain. Energy Rev.* 120, 109627. <https://doi.org/10.1016/j.rser.2019.109627>.
12. Tu, Y., Wang, R., Zhang, Y., and Wang, J. (2018). Progress and expectation of atmospheric water harvesting. *Joule* 2, 1452–1475. <https://doi.org/10.1016/j.joule.2018.07.015>.
13. Oki, T., and Kanae, S. (2006). Global hydrological cycles and world water resources. *Science* 313, 1068–1072.
14. Zhou, X., Lu, H., Zhao, F., and Yu, G. (2020). Atmospheric water harvesting: a review of material and structural designs. *ACS Mater. Lett.* 2, 671–684. <https://doi.org/10.1021/acsmaterialslett.0c00130>.
15. Lu, H., Shi, W., Guo, Y., Guan, W., Lei, C., and Yu, G. (2022). Materials engineering for atmospheric water harvesting: progress and perspectives. *Adv. Mater.* 34, e2110079. <https://doi.org/10.1002/adma.202110079>.
16. Yang, K., Pan, T., Lei, Q., Dong, X., Cheng, Q., and Han, Y. (2021). A roadmap to sorption-based atmospheric water harvesting: from molecular sorption mechanism to sorbent design and system optimization. *Environ. Sci. Technol.* 55, 6542–6560. <https://doi.org/10.1021/acs.est.1c00257>.
17. Ejeian, M., and Wang, R.Z. (2021). Adsorption-based atmospheric water harvesting. *Joule* 5, 1678–1703. <https://doi.org/10.1016/j.joule.2021.04.005>.
18. Zhang, Y., Nandakumar, D.K., and Tan, S.C. (2020). Digestion of ambient humidity for energy generation. *Joule* 4, 2532–2536. <https://doi.org/10.1016/j.joule.2020.10.003>.
19. LaPotin, A., Kim, H., Rao, S.R., and Wang, E.N. (2019). Adsorption-based atmospheric water harvesting: impact of material and component properties on system-level performance. *Acc. Chem. Res.* 52, 1588–1597. <https://doi.org/10.1021/acs.accounts.9b00062>.
20. Zhuang, S., Qi, H., Wang, X., Li, X., Liu, K., Liu, J., and Zhang, H. (2020). Advances in solar-driven hygroscopic water harvesting. *Glob. Chall.* 5, 2000085. <https://doi.org/10.1002/gch2.202000085>.
21. Wang, B., Zhou, X., Guo, Z., and Liu, W. (2021). Recent advances in atmosphere water harvesting: design principle, materials, devices, and applications. *Nano Today* 40, 101283. <https://doi.org/10.1016/j.nantod.2021.101283>.
22. Peeters, R., Vanderschaeghe, H., Rongé, J., and Martens, J.A. (2020). Energy performance and climate dependency of technologies for fresh water production from atmospheric water vapour. *Environ. Sci. Water Res. Technol.* 6, 2016–2034. <https://doi.org/10.1039/d0ew00128g>.
23. Bai, H., Wang, L., Ju, J., Sun, R., Zheng, Y., and Jiang, L. (2014). Efficient water collection on integrative bioinspired surfaces with star-shaped wettability patterns. *Adv. Mater.* 26, 5025–5030. <https://doi.org/10.1002/adma.201400262>.
24. Park, K.C., Kim, P., Grinthal, A., He, N., Fox, D., Weaver, J.C., and Aizenberg, J. (2016). Condensation on slippery asymmetric bumps. *Nature* 531, 78–82. <https://doi.org/10.1038/nature16956>.
25. Ahmed, E.M. (2015). Hydrogel: preparation, characterization, and applications: a review. *J. Adv. Res.* 6, 105–121. <https://doi.org/10.1016/j.jare.2013.07.006>.
26. Zhao, F., Bae, J., Zhou, X., Guo, Y., and Yu, G. (2018). Nanostructured functional hydrogels as an emerging platform for advanced energy technologies. *Adv. Mater.* 30, e1801796. <https://doi.org/10.1002/adma.201801796>.
27. Zhou, X., Guo, Y., Zhao, F., and Yu, G. (2019). Hydrogels as an emerging material platform for solar water purification. *Acc. Chem. Res.* 52, 3244–3253. <https://doi.org/10.1021/acs.accounts.9b00455>.
28. Zhao, F., Shi, Y., Pan, L., and Yu, G. (2017). Multifunctional nanostructured conductive polymer gels: synthesis, properties, and applications. *Acc. Chem. Res.* 50, 1734–1743. <https://doi.org/10.1021/acs.accounts.7b00191>.
29. Wang, C., Hua, L., Yan, H., Li, B., Tu, Y., and Wang, R. (2020). A thermal management strategy for electronic devices based on moisture sorption-desorption processes. *Joule* 4, 435–447. <https://doi.org/10.1016/j.joule.2019.12.005>.
30. Yao, H., Zhang, P., Huang, Y., Cheng, H., Li, C., and Qu, L. (2020). Highly efficient clean water production from contaminated air with a wide humidity range. *Adv. Mater.* 32, 1905875. <https://doi.org/10.1002/adma.201905875>.
31. Yang, K., Pan, T., Pinnau, I., Shi, Z., and Han, Y. (2020). Simultaneous generation of atmospheric water and electricity using a hygroscopic aerogel with fast sorption kinetics. *Nano Energy* 78, 105326. <https://doi.org/10.1016/j.nanoen.2020.105326>.
32. Nandakumar, D.K., Zhang, Y., Ravi, S.K., Guo, N., Zhang, C., and Tan, S.C. (2019). Solar energy triggered clean water harvesting from humid air existing above sea surface enabled by a hydrogel with ultrahigh hygroscopicity. *Adv. Mater.* 31, 1806730. <https://doi.org/10.1002/adma.201806730>.
33. Chua, H.T., Ng, K.C., Chakraborty, A., Oo, N.M., and Othman, M.A. (2002). Adsorption characteristics of silica gel + water systems. *J. Chem. Eng. Data* 47, 1177–1181. <https://doi.org/10.1021/je0255067>.
34. Yang, J., Zhang, X., Qu, H., Yu, Z.G., Zhang, Y., Eey, T.J., Zhang, Y.W., and Tan, S.C. (2020). A moisture-hungry copper complex harvesting air moisture for potable water and autonomous urban agriculture. *Adv. Mater.* 32, e2002936. <https://doi.org/10.1002/adma.202002936>.
35. Zhang, X., Yang, J., Borayek, R., Qu, H., Nandakumar, D.K., Zhang, Q., Ding, J., and Tan, S.C. (2020). Super-hygroscopic film for wearables with dual functions of expediting sweat evaporation and energy harvesting. *Nano Energy* 75, 104873. <https://doi.org/10.1016/j.nanoen.2020.104873>.
36. Li, R., Shi, Y., Alsaedi, M., Wu, M., Shi, L., and Wang, P. (2018). Hybrid hydrogel with high water vapor harvesting capacity for deployable solar-driven atmospheric water generator. *Environ. Sci. Technol.* 52, 11367–11377. <https://doi.org/10.1021/acs.est.8b02852>.
37. Kallenberger, P.A., and Fröba, M. (2018). Water harvesting from air with a hygroscopic salt in a hydrogel-derived matrix. *Commun.*

- Chem. 1, 28. <https://doi.org/10.1038/s42004-018-0028-9>.
38. Lei, C., Guo, Y., Guan, W., Lu, H., Shi, W., and Yu, G. (2022). Polyzwitterionic hydrogels for efficient atmospheric water harvesting. *Angew. Chem. Int. Ed. Engl.* 61, e202200271. <https://doi.org/10.1002/anie.202200271>.
  39. Xu, J., Li, T., Yan, T., Wu, S., Wu, M., Chao, J., Huo, X., Wang, P., and Wang, R. (2021). Ultrahigh solar-driven atmospheric water production enabled by scalable rapid-cycling water harvester with vertically aligned nanocomposite sorbent. *Energy Environ. Sci.* 14, 5979–5994. <https://doi.org/10.1039/d1ee01723c>.
  40. Entezari, A., Ejeian, M., and Wang, R. (2020). Super atmospheric water harvesting hydrogel with alginate chains modified with binary salts. *ACS Mater. Lett.* 2, 471–477. <https://doi.org/10.1021/acsmaterialslett.9b00315>.
  41. Wu, M., Li, R., Shi, Y., Altunkaya, M., Aleid, S., Zhang, C., Wang, W., and Wang, P. (2021). Metal- and halide-free, solid-state polymeric water vapor sorbents for efficient water-sorption-driven cooling and atmospheric water harvesting. *Mater. Horiz.* 8, 1518–1527. <https://doi.org/10.1039/d0mh02051f>.
  42. Zhao, F., Zhou, X., Liu, Y., Shi, Y., Dai, Y., and Yu, G. (2019). Super moisture-absorbent gels for all-weather atmospheric water harvesting. *Adv. Mater.* 31, 1806446. <https://doi.org/10.1002/adma.201806446>.
  43. Yilmaz, G., Meng, F.L., Lu, W., Abed, J., Peh, C.K.N., Gao, M., Sargent, E.H., and Ho, G.W. (2020). Autonomous atmospheric water seeping MOF matrix. *Sci. Adv.* 6, eabc8605. <https://doi.org/10.1126/sciadv.abc8605>.
  44. Ni, F., Qiu, N., Xiao, P., Zhang, C., Jian, Y., Liang, Y., Xie, W., Yan, L., and Chen, T. (2020). Tillandsia-inspired hygroscopic photothermal organogels for efficient atmospheric water harvesting. *Angew. Chem. Int. Ed. Engl.* 59, 19237–19246. <https://doi.org/10.1002/anie.202007885>.
  45. Ni, F., Xiao, P., Zhang, C., Zhou, W., Depeng, L., Kuo, S.-W., and Chen, T. (2021). Atmospheric hygroscopic ionogels with dynamically stable cooling interfaces enable a durable thermoelectric performance enhancement. *Adv. Mater.* 33, 2103937.
  46. Coasne, B., Galarneau, A., Pellenq, R.J.M., and Di Renzo, F. (2013). Adsorption, intrusion and freezing in porous silica: the view from the nanoscale. *Chem. Soc. Rev.* 42, 4141–4171. <https://doi.org/10.1039/c2cs35384a>.
  47. Nandakumar, D.K., Ravi, S.K., Zhang, Y., Guo, N., Zhang, C., and Tan, S.C. (2018). A super hygroscopic hydrogel for harnessing ambient humidity for energy conservation and harvesting. *Energy Environ. Sci.* 11, 2179–2187. <https://doi.org/10.1039/c8ee00902c>.
  48. Kalmutzki, M.J., Diercks, C.S., and Yaghi, O.M. (2018). Metal-organic frameworks for water harvesting from air. *Adv. Mater.* 30, e1704304. <https://doi.org/10.1002/adma.201704304>.
  49. de Lange, M.F., Verouden, K.J.F.M., Vlugt, T.J.H., Gascon, J., and Kapteijn, F. (2015). Adsorption-driven heat pumps: the potential of metal-organic frameworks. *Chem. Rev.* 115, 12205–12250. <https://doi.org/10.1021/acs.chemrev.5b00059>.
  50. Canivet, J., Fateeva, A., Guo, Y., Coasne, B., and Farrusseng, D. (2014). Water adsorption in MOFs: fundamentals and applications. *Chem. Soc. Rev.* 43, 5594–5617. <https://doi.org/10.1039/c4cs00078a>.
  51. Thommes, M., Kaneko, K., Neimark, A.V., Olivier, J.P., Rodriguez-Reinoso, F., Rouquerol, J., and Sing, K.S. (2015). Physisorption of gases, with special reference to the evaluation of surface area and pore size distribution (IUPAC technical report). *Pure Appl. Chem.* 87, 1051–1069. <https://doi.org/10.1515/pac-2014-1117>.
  52. Lin, K.F., and Yeh, R.J. (2002). Moisture absorption behavior of rubber-modified epoxy resins. *J. Appl. Polym. Sci.* 86, 3718–3724. <https://doi.org/10.1002/app.11432>.
  53. Díaz-Marín, C.D., Zhang, L., Lu, Z., Alshrah, M., Grossman, J.C., and Wang, E.N. (2022). Kinetics of sorption in hygroscopic hydrogels. *Nano Lett.* 22, 1100–1107. <https://doi.org/10.1021/acs.nanolett.1c04216>.
  54. Zhao, W., Hsu, S.L., Ravichandran, S., and Bonner, A.M. (2019). Moisture effects on the physical properties of cross-linked phenolic resins. *Macromolecules* 52, 3367–3375. <https://doi.org/10.1021/acs.macromol.9b00385>.
  55. Zhou, J., Wu, C., Wu, D., Wang, Q., and Chen, Y. (2018). Humidity-sensitive polymer xerogel actuators prepared by biaxial pre-stretching and drying. *Chem. Commun.* 54, 11610–11613. <https://doi.org/10.1039/c8cc06750c>.
  56. Ge, Y., Wang, H., Xue, J., Jiang, J., Liu, Z., Liu, Z., Li, G., and Zhao, Y. (2021). Programmable humidity-responsive actuation of polymer films enabled by combining shape memory property and surface-tunable hygroscopicity. *ACS Appl. Mater. Interfaces* 13, 38773–38782. <https://doi.org/10.1021/acsami.1c11862>.
  57. Shrestha, M., Lu, Z., and Lau, G.-K. (2021). High humidity sensing by 'hygomorphic' dielectric elastomer actuator. *Sens. Actuators B-Chem.* 329, 129268. <https://doi.org/10.1016/j.snb.2020.129268>.
  58. Thiangtham, S., Runt, J., and Manuspiya, H. (2019). Sulfonation of dialdehyde cellulose extracted from sugarcane bagasse for synergistically enhanced water solubility. *Carbohydr. Polym.* 208, 314–322. <https://doi.org/10.1016/j.carbpol.2018.12.080>.
  59. Yang, L., Ravi, S.K., Nandakumar, D.K., Alzakia, F.I., Lu, W., Zhang, Y., Yang, J., Zhang, Q., Zhang, X., and Tan, S.C. (2019). A hybrid artificial photocatalysis system splits atmospheric water for simultaneous dehumidification and power generation. *Adv. Mater.* 31, e1902963. <https://doi.org/10.1002/adma.201902963>.
  60. Yang, L., Nandakumar, D.K., Miao, L., Suresh, L., Zhang, D., Xiong, T., Vaghiasya, J.V., Kwon, K.C., and Ching Tan, S. (2020). Energy harvesting from atmospheric humidity by a hydrogel-integrated ferroelectric-semiconductor system. *Joule* 4, 176–188. <https://doi.org/10.1016/j.joule.2019.10.008>.
  61. Kim, Y., Hendrickson, R., Mosier, N., Hilaly, A., and Ladisch, M.R. (2011). Cassava starch pearls as a desiccant for drying ethanol. *Ind. Eng. Chem. Res.* 50, 8678–8685. <https://doi.org/10.1021/ie2003297>.
  62. Qiao, D., Yu, L., Bao, X., Zhang, B., and Jiang, F. (2017). Understanding the microstructure and absorption rate of starch-based superabsorbent polymers prepared under high starch concentration. *Carbohydr. Polym.* 175, 141–148. <https://doi.org/10.1016/j.carbpol.2017.07.071>.
  63. Thijs, H.M.L., Becer, C.R., Guerrero-Sanchez, C., Fournier, D., Hoogenboom, R., and Schubert, U.S. (2007). Water uptake of hydrophilic polymers determined by a thermal gravimetric analyzer with a controlled humidity chamber. *J. Mater. Chem.* 17, 4864. <https://doi.org/10.1039/b711990a>.
  64. Kim, S.J., Kim, S.I., Lee, K.B., Park, Y.D., and Lee, K.J. (2003). Sorption characterization of poly(vinyl alcohol)/chitosan interpenetrating polymer network hydrogels. *J. Appl. Polym. Sci.* 90, 86. <https://doi.org/10.1002/app.12540>.
  65. Lewis, G., and America, M. (2009). Technology for Drying Resin. <https://knowledge.ulprospector.com/1551/pe-technology-drying-resin/>.
  66. Riza, M.A., Go, Y.I., Maier, R.R.J., Harun, S.W., and Anas, S.B. (2020). Hygroscopic materials and characterization techniques for fiber sensing applications: a review. *Sens. Mater.* 32, 3755–3772. <https://doi.org/10.18494/sam.2020.2967>.
  67. Wang, W., Yao, L., Cheng, C.-Y., Zhang, T., Atsumi, H., Wang, L., Wang, G., Anilionyte, O., Steiner, H., Ou, J., et al. (2017). Harnessing the hygroscopic and biofluorescent behaviors of genetically tractable microbial cells to design biohybrid wearables. *Sci. Adv.* 3, e1601984. <https://doi.org/10.1126/sciadv.1601984>.
  68. Wang, Z., Liu, M.c., Chang, Z.-y., and Li, H.-b. (2021). Study on the graft modification mechanism of macroporous silica gel surface based on silane coupling agent vinyl triethoxysilane. *RSC Adv.* 11, 25158–25169. <https://doi.org/10.1039/d1ra04296c>.
  69. Burch, N.C., Jasuja, H., and Walton, K.S. (2014). Water stability and adsorption in metal-organic frameworks. *Chem. Rev.* 114, 10575–10612. <https://doi.org/10.1021/cr5002589>.
  70. Yang, Y., Rana, D., and Lan, C.Q. (2015). Development of solid super desiccants based on a polymeric superabsorbent hydrogel composite. *RSC Adv.* 5, 59583–59590. <https://doi.org/10.1039/c5ra04346h>.
  71. Li, R., Shi, Y., Wu, M., Hong, S., and Wang, P. (2020). Photovoltaic panel cooling by atmospheric water sorption–evaporation cycle. *Nat. Sustain.* 3, 636–643. <https://doi.org/10.1038/s41893-020-0535-4>.
  72. Zhou, X., Zhang, P., Zhao, F., and Yu, G. (2020). Super moisture absorbent gels for sustainable agriculture via atmospheric water irrigation. *ACS Mater. Lett.* 2, 1419–1422. <https://doi.org/10.1021/acsmaterialslett.0c00439>.
  73. Pu, S., Fu, J., Liao, Y., Ge, L., Zhou, Y., Zhang, S., Zhao, S., Liu, X., Hu, X., Liu, K., and Chen, J.

- (2020). Promoting energy efficiency via a self-adaptive evaporative cooling hydrogel. *Adv. Mater.* **32**, 1907307.
74. Yang, P., Feng, C., Liu, Y., Cheng, T., Yang, X., Liu, H., Liu, K., and Fan, H.J. (2020). Thermal self-protection of zinc-ion batteries enabled by smart hygroscopic hydrogel electrolytes. *Adv. Energy Mater.* **10**, 2002898.
75. Pu, S., Liao, Y., Chen, K., Fu, J., Zhang, S., Ge, L., Conta, G., Bouzarif, S., Cheng, T., Hu, X., et al. (2020). Thermogalvanic hydrogel for synchronous evaporative cooling and low-grade heat energy harvesting. *Nano Lett.* **20**, 3791–3797. <https://doi.org/10.1021/acs.nanolett.0c00800>.
76. Yan, T., Li, T., Xu, J., Chao, J., Wang, R., Aristov, Y.I., Gordeeva, L.G., Dutta, P., and Murthy, S.S. (2021). Ultrahigh-energy-density sorption thermal battery enabled by graphene aerogel-based composite sorbents for thermal energy harvesting from air. *ACS Energy Lett.* **6**, 1795–1802. <https://doi.org/10.1021/acsenerylett.1c00284>.
77. Aleid, S., Wu, M., Li, R., Wang, W., Zhang, C., Zhang, L., and Wang, P. (2022). Salting-in effect of zwitterionic polymer hydrogel facilitates atmospheric water harvesting. *ACS Mater. Lett.* **4**, 511–520. <https://doi.org/10.1021/acsmaterialslett.1c00723>.
78. Qi, H., Wei, T., Zhao, W., Zhu, B., Liu, G., Wang, P., Lin, Z., Wang, X., Li, X., Zhang, X., and Zhu, J. (2019). An interfacial solar-driven atmospheric water generator based on a liquid sorbent with simultaneous adsorption-desorption. *Adv. Mater.* **31**, 1903378. <https://doi.org/10.1002/adma.201903378>.
79. Forney, C.F., and Brandl, D.G. (1992). Control of humidity in small controlled-environment chambers using glycerol-water solutions. *Horttechnology* **2**, 52–54. <https://doi.org/10.21273/horttech.2.1.52>.
80. Wang, X., Li, X., Liu, G., Li, J., Hu, X., Xu, N., Zhao, W., Zhu, B., and Zhu, J. (2019). An interfacial solar heating assisted liquid sorbent atmospheric water generator. *Angew. Chem. Int. Ed. Engl.* **58**, 12054–12058. <https://doi.org/10.1002/anie.201905229>.
81. Tran, C.D., De Paoli Lacerda, S.H., Lacerda, P., and Oliveira, D. (2003). Absorption of water by room-temperature ionic liquids: effect of anions on concentration and state of water. *Appl. Spectrosc.* **57**, 152–157. <https://doi.org/10.1366/000370203321535051>.
82. Rieth, A.J., Yang, S., Wang, E.N., and Dinca, M. (2017). Record atmospheric fresh water capture and heat transfer with a material operating at the water uptake reversibility limit. *ACS Cent. Sci.* **3**, 668–672. <https://doi.org/10.1021/acscentsci.7b00186>.
83. Yang, L., Loh, L., Nandakumar, D.K., Lu, W., Gao, M., Wee, X.L.C., Zeng, K., Bosman, M., and Tan, S.C. (2020). Sustainable fuel production from ambient moisture via ferroelectrically driven MoS<sub>2</sub> nanosheets. *Adv. Mater.* **32**, e2000971. <https://doi.org/10.1002/adma.202000971>.
84. Xue, J., Zhao, F., Hu, C., Zhao, Y., Luo, H., Dai, L.M., Qu, L., and Qu, L.T. (2016). Vapor-activated power generation on conductive polymer. *Adv. Funct. Mater.* **26**, 8784–8792. <https://doi.org/10.1002/adfm.201604188>.
85. He, P., Wu, J., Pan, X., Chen, L., Liu, K., Gao, H., Wu, H., Cao, S., Huang, L., and Ni, Y. (2020). Anti-freezing and moisturizing conductive hydrogels for strain sensing and moist-electric generation applications. *J. Mater. Chem. A* **8**, 3109–3118. <https://doi.org/10.1039/c9ta12940e>.
86. Mandal, S., Roy, S., Mandal, A., Ghoshal, T., Das, G., Singh, A., and Goswami, D.K. (2020). Protein-based flexible moisture-induced energy-harvesting devices as self-biased electronic sensors. *ACS Appl. Electron. Mater.* **2**, 780–789. <https://doi.org/10.1021/acsaelm.9b00842>.
87. Li, M., Zong, L., Yang, W., Li, X., You, J., Wu, X., Li, Z., and Li, C. (2019). Biological nanofibrous generator for electricity harvest from moist air flow. *Adv. Funct. Mater.* **29**, 1901798.
88. Matsumoto, K., Sakikawa, N., and Miyata, T. (2018). Thermo-responsive gels that absorb moisture and ooze water. *Nat. Commun.* **9**, 2315. <https://doi.org/10.1038/s41467-018-04810-8>.
89. Cho, J., and Goodson, K.E. (2015). Thermal transport: cool electronics. *Nat. Mater.* **14**, 136–137. <https://doi.org/10.1038/nmat4194>.
90. Yu, W., Zhang, G., Liu, C., and Fan, S. (2020). Hard carbon nanotube sponges for highly efficient cooling via moisture absorption-desorption process. *ACS Nano* **14**, 14091–14099. <https://doi.org/10.1021/acsnano.0c06748>.
91. Shen, D., Duley, W.W., Peng, P., Xiao, M., Feng, J., Liu, L., Zou, G., and Zhou, Y.N. (2020). Moisture-enabled electricity generation: from physics and materials to self-powered applications. *Adv. Mater.* **32**, e2003722. <https://doi.org/10.1002/adma.202003722>.
92. Xiao, P., He, J., Ni, F., Zhang, C., Liang, Y., Zhou, W., Gu, J., Xia, J., Kuo, S.-W., and Chen, T. (2020). Exploring interface confined water flow and evaporation enables solar-thermal-electro integration towards clean water and electricity harvest via asymmetric functionalization strategy. *Nano Energy* **68**, 104385. <https://doi.org/10.1016/j.nanoen.2019.104385>.
93. Tao, P., Ni, G., Song, C.Y., Shang, W., Wu, J.B., Zhu, J., Chen, G., and Deng, T. (2018). Solar-driven interfacial evaporation. *Nat. Energy* **3**, 1031–1041. <https://doi.org/10.1038/s41560-018-0260-7>.
94. Chen, C., Kuang, Y., and Hu, L. (2019). Challenges and opportunities for solar evaporation. *Joule* **3**, 683–718. <https://doi.org/10.1016/j.joule.2018.12.023>.
95. Zhao, F., Guo, Y., Zhou, X., Shi, W., and Yu, G. (2020). Materials for solar-powered water evaporation. *Nat. Rev. Mater.* **5**, 388–401. <https://doi.org/10.1038/s41578-020-0182-4>.
96. Gu, J., Xiao, P., Chen, P., Zhang, L., Wang, H., Dai, L., Song, L., Huang, Y., Zhang, J., and Chen, T. (2017). Functionalization of biodegradable PLA nonwoven fabric as superoleophilic and superhydrophobic material for efficient oil absorption and oil/water separation. *ACS Appl. Mater. Interfaces* **9**, 5968–5973. <https://doi.org/10.1021/acsaami.6b13547>.
97. Zhang, L., Zha, X., Zhang, G., Gu, J., Zhang, W., Huang, Y., Zhang, J., and Chen, T. (2018). Designing a reductive hybrid membrane to selectively capture noble metallic ions during oil/water emulsion separation with further function enhancement. *J. Mater. Chem. A* **6**, 10217–10225. <https://doi.org/10.1039/c8ta01864b>.
98. Gu, J., Ji, L., Xiao, P., Zhang, C., Li, J., Yan, L., and Chen, T. (2021). Recent progress in superhydrophilic carbon-based composite membranes for oil/water emulsion separation. *ACS Appl. Mater. Interfaces* **13**, 36679–36696. <https://doi.org/10.1021/acsaami.1c07737>.
99. Xia, J., Xiao, P., Gu, J., Chen, T., Liu, C., Yan, L., and Chen, T. (2020). Interfacial self-assembled GR/GO ultrathin membranes on A large scale for molecular sieving. *J. Mater. Chem. A* **8**, 18735–18744. <https://doi.org/10.1039/d0ta05337f>.
100. Zhang, X., Xu, J., Du, M., and Zhang, Y. (2012). *In Sustainable Development of Urban Environment and Building Material*, Pts 1-4, 374, H. Li, Y.F. Liu, M. Guo, R. Zhang, and J. Du, eds., p. 1021.
101. Wang, W., Shi, Y., Zhang, C., Li, R., Wu, M., Zhuo, S., Aleid, S., and Wang, P. (2021). Solar seawater distillation by flexible and fully passive multistage membrane distillation. *Nano Lett.* **21**, 5068–5074. <https://doi.org/10.1021/acs.nanolett.1c00910>.
102. Gao, M., Peh, C.K., Meng, F.L., and Ho, G.W. (2021). Photothermal membrane distillation toward solar water production. *Small Methods* **5**, e2001200. <https://doi.org/10.1002/smt.202001200>.
103. Xiao, P., Gu, J., Zhang, C., Ni, F., Liang, Y., He, J., Zhang, L., Ouyang, J., Kuo, S.W., and Chen, T. (2019). A scalable, low-cost and robust photo-thermal fabric with tunable and programmable 2D/3D structures towards environmentally adaptable liquid/solid-medium water extraction. *Nano Energy* **65**, 104002. <https://doi.org/10.1016/j.nanoen.2019.104002>.
104. Ni, F., Xiao, P., Qiu, N., Zhang, C., Liang, Y., Gu, J., Xia, J., Zeng, Z., Wang, L., Xue, Q., and Chen, T. (2019). Collective behaviors mediated multifunctional black sand aggregate towards environmentally adaptive solar-to-thermal purified water harvesting. *Nano Energy* **68**, 104311. <https://doi.org/10.1016/j.nanoen.2019.104311>.
105. Zhang, C., Xiao, P., Ni, F., Yang, Y., Gu, J., Zhang, L., Xia, J., Huang, Y., Wang, W., and Chen, T. (2019). Programmable interface asymmetric integration of carbon nanotubes and gold nanoparticles toward flexible, configurable, and surface-enhanced Raman scattering active all-in-one solar-driven evaporators. *Energy Technol.* **7**, 1900787.
106. Zhang, C., Xiao, P., Ni, F., Yan, L., Liu, Q., Zhang, D., Gu, J., Wang, W., and Chen, T. (2020). Converting pomelo peel into eco-friendly and low-consumption photothermal biomass sponge toward multifunctional solar-to-heat conversion. *ACS Sustain. Chem. Eng.*

- 8, 5328–5337. <https://doi.org/10.1021/acssuschemeng.0c00681>.
107. Ni, F., Xiao, P., Zhang, C., Liang, Y., Gu, J., Zhang, L., and Chen, T. (2019). Micro-/Macroscopically synergetic control of switchable 2D/3D photothermal water purification enabled by robust, portable, and cost-effective cellulose papers. *ACS Appl. Mater. Interfaces* **11**, 15498–15506. <https://doi.org/10.1021/acami.9b00380>.
108. Xiao, P., He, J., Liang, Y., Zhang, C., Gu, J., Zhang, J., Huang, Y., Kuo, S.W., and Chen, T. (2019). Rationally programmable paper-based artificial trees toward multipath solar-driven water extraction from liquid/solid substrates. *Solar RRL* **3**, 1900004. <https://doi.org/10.1002/solr.201900004>.
109. Zhang, C., Xiao, P., Ni, F., Gu, J., Chen, J., Nie, Y., Kuo, S.-W., and Chen, T. (2022). Breathable and superhydrophobic photothermic fabric enables efficient interface energy management via confined heating strategy for sustainable seawater evaporation. *Chem. Eng. J.* **428**, 131142. <https://doi.org/10.1016/j.cej.2021.131142>.
110. Zhou, L., Tan, Y., Wang, J., Xu, W., Yuan, Y., Cai, W., Zhu, S., and Zhu, J. (2016). 3D self-assembly of aluminium nanoparticles for plasmon-enhanced solar desalination. *Nat. Photonics* **10**, 393–398. <https://doi.org/10.1038/nphoton.2016.75>.
111. Dao, V.D., and Choi, H.-S. (2018). Carbon-based sunlight absorbers in solar-driven steam generation devices. *Glob. Chall.* **2**, 201700094. <https://doi.org/10.1002/gch2.201700094>.
112. Gao, M., Zhu, L., Peh, C.K., and Ho, G.W. (2019). Solar absorber material and system designs for photothermal water vaporization towards clean water and energy production. *Energy Environ. Sci.* **12**, 841–864. <https://doi.org/10.1039/c8ee01146j>.
113. Zhou, X., Zhao, F., Guo, Y., Yu, G.H., and Yu, G. (2019). Architecting highly hydratable polymer networks to tune the water state for solar water purification. *Sci. Adv.* **5**, eaaw5484. <https://doi.org/10.1126/sciadv.aaw5484>.
114. Huang, J., Yu, H., Guan, X., Wang, G., and Guo, R. (2015). Accelerated dryland expansion under climate change. *Nat. Clim. Change* **6**, 166–171. <https://doi.org/10.1038/nclimate2837>.
115. Food and Agriculture Organization of the United Nations (2017). *Water for Sustainable Food and Agriculture: A Report Produced for the G20 Presidency of Germany (Food and Agriculture Organization of the United Nations)*.
116. Puy, A., Borgonovo, E., Lo Piano, S., Levin, S.A., and Saltelli, A. (2021). Irrigated areas drive irrigation water withdrawals. *Nat. Commun.* **12**, 4525. <https://doi.org/10.1038/s41467-021-24508-8>.
117. Zhu, L.L., Gao, M.M., Peh, C.K.N., Wang, X.Q., and Ho, G.W. (2018). Self-contained monolithic carbon sponges for solar-driven interfacial water evaporation distillation and electricity generation. *Adv. Energy Mater.* **8**, 1702149. <https://doi.org/10.1002/aenm.201702149>.
118. Zhu, L.L., Ding, T.P., Gao, M.M., Peh, C.K.N., and Ho, G.W. (2019). Shape conformal and thermal insulative organic solar absorber sponge for photothermal water evaporation and thermoelectric power generation. *Adv. Energy Mater.* **9**, 1900250.
119. Xu, N., Zhu, P., Sheng, Y., Zhou, L., Li, X., Tan, H., Zhu, S., and Zhu, J. (2020). Synergistic tandem solar electricity-water generators. *Joule* **4**, 347–358. <https://doi.org/10.1016/j.joule.2019.12.010>.
120. Ding, T., and Ho, G.W. (2021). Using the sun to Co-generate electricity and freshwater. *Joule* **5**, 1639–1641. <https://doi.org/10.1016/j.joule.2021.06.021>.
121. Gordeeva, L.G., Tu, Y.D., Pan, Q., Palash, M.L., Saha, B.B., Aristov, Y.I., and Wang, R.Z. (2021). Metal-organic frameworks for energy conversion and water harvesting: a bridge between thermal engineering and material science. *Nano Energy* **84**, 105946. <https://doi.org/10.1016/j.nanoen.2021.105946>.